Electronic Supplementary Material (ESI) for Green Chemistry.

Supporting Information

Maximizing ionic liquid content and specific surface area in hierarchically nanoporous hypercrosslinked poly(ionic liquid)s towards efficient conversion of CO_2 into cyclic carbonates

Hongbing Lyu, [a] Xiaochen Wang,*[a] Wanting Sun, [a] Ergang Xu, [a] Yaping She, [a] Anqiu Liu,*[a] Daming Gao, [a] Miao Hu, [a] Jianhua Guo, [a] Kunhong Hu, [a] Jihai Cheng, [a] Zhouyang Long, [b] Yangqing Liu [c] and Pengjie Zhang [d]

[a] School of Energy Materials and Chemical Engineering, Hefei University, Hefei 230601, China
[b] School of Chemistry and Materials Science, Jiangsu Key Laboratory of Green Synthetic Chemistry for Functional Materials, Jiangsu Normal University, Xuzhou 221116, China
[c] School of Chemistry and Chemical Engineering, Yancheng Institute of Technology, Yancheng 224000, China
[d] BGRIMM Technology Group Co, Ltd, Beijing 102600, China

Corresponding Authors
* Tel: +86-551-62158395
E-mail: wxc@hfuu.edu.cn (X. Wang); liuaq@hfuu.edu.cn (A. Liu)

Synthesis and characterization of imidazolium-based ionic liquid monomers

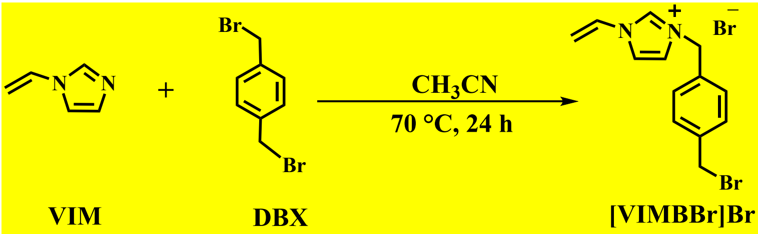

[VIMBBr]Br: ^{1}H NMR (400 MHz, D_2O) (Figure S1A): δ=8.94 (s, 1H), 7.68 (t, 1H), 7.47 (t, 1H), 7.40 (m, 4H), 5.71 (q, 2H), 5.38 (t, 3H), 4.56 (s, 2H). ^{13}C NMR (100 MHz, D_2O) (Figure S1B): δ=141.4, 134.5, 132.4, 129.0, 128.1, 122.8, 119.7, 109.5, 63.3, 52.9.

Scheme S1. Synthesis of the benzylbromide-tethered IL [VIMBBr]Br.

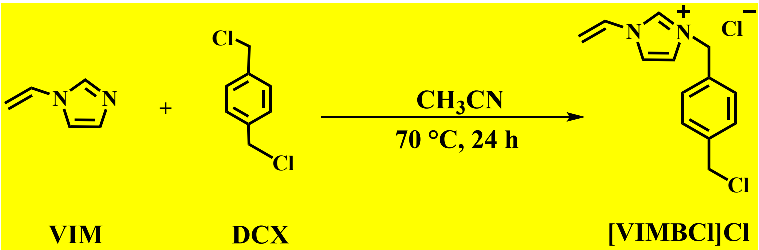

[VIMBCl]Cl: ^{1}H NMR (400 MHz, D_2O) (Figure S2A): δ=8.93 (d, 1H),7.65 (d, 1H), 7.43 (d, 1H),7.32 (d, 4H), 5.68(q, 2H), 5.31 (q, 3H), 4.57 (t, 2H). ^{13}C NMR (100 MHz, D_2O) (Figure S2B): δ=139.1, 134.5, 133.3, 129.6, 129.2, 128.1, 122.8, 119.8, 109.6, 52.7, 45.5.

Scheme S2. Synthesis of the benzylchloride-tethered IL [VIMBCl]Cl.

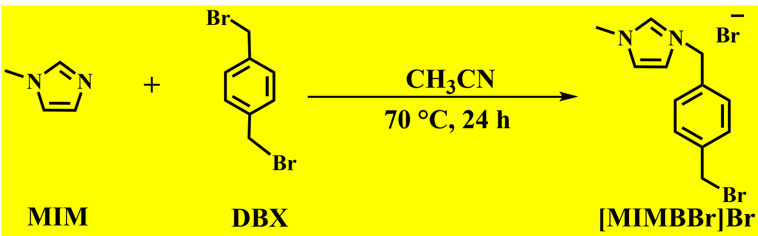

[MIMBBr]Br: ^{1}H NMR (400 MHz, D_2O) (Figure S3A): δ=8.59 (s, 1H), 7.42 (d, 2H), 7.33 (m, 4H), 5.28 (t, 2H), 4.52 (t, 2H), 3.74 (s, 2H). ^{13}C NMR (100 MHz, D_2O) (Figure S3 B): δ=141.1, 136.0, 132.8, 128.7, 123.6, 122.1, 63.3, 52.4, 35.6.

Scheme S3. Synthesis of the benzylbromide-tethered IL [MIMBBr]Br.

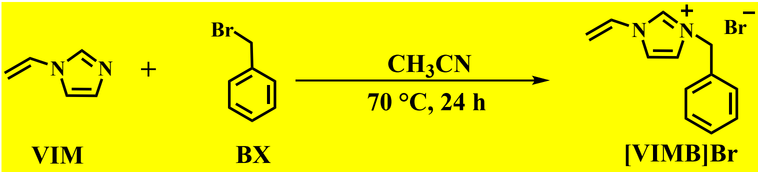

[VIMB]Br: ^{1}H NMR (400 MHz, D_2O) (Figure S4A): δ= 7.65 (d, 1H), 7.43 (d, 1H), 7.37(q, 4H), 7.01 (q, 1H), 5.68 (q, 2H), 5.31 (q, 4H). ^{13}C NMR (100 MHz, D_2O) (Figure S4B) δ=129.3, 129.3, 128.6, 128.1, 122.7, 119.6, 109.4, 53.1.

Scheme S4. Synthesis of the benzyl-tethered IL [VIMB]Br.

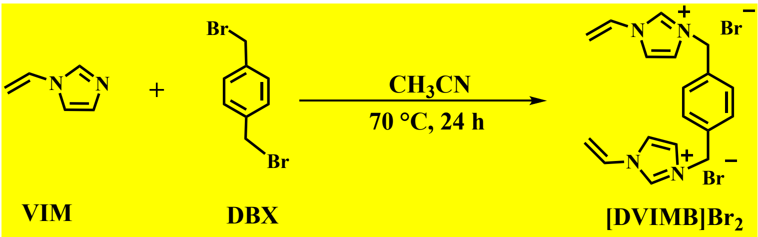

[DVIMB]Br_2: ^{1}H NMR (400 MHz, D_2O) (Figure S5A): δ=7.67 (d, 2H), 7.43 (d, 4H), 7.36 (s,4H), 5.69 (t, 2H), 5.34 (t, 4H). ^{13}C NMR (100 MHz, D_2O) (Figure S5B) δ=134.2, 129. 4, 128.0, 122.8, 119.7, 109.5, 52.5.

Scheme S5. Synthesis of the bis-vinylimidazolium IL [DVIMB]Br_2.

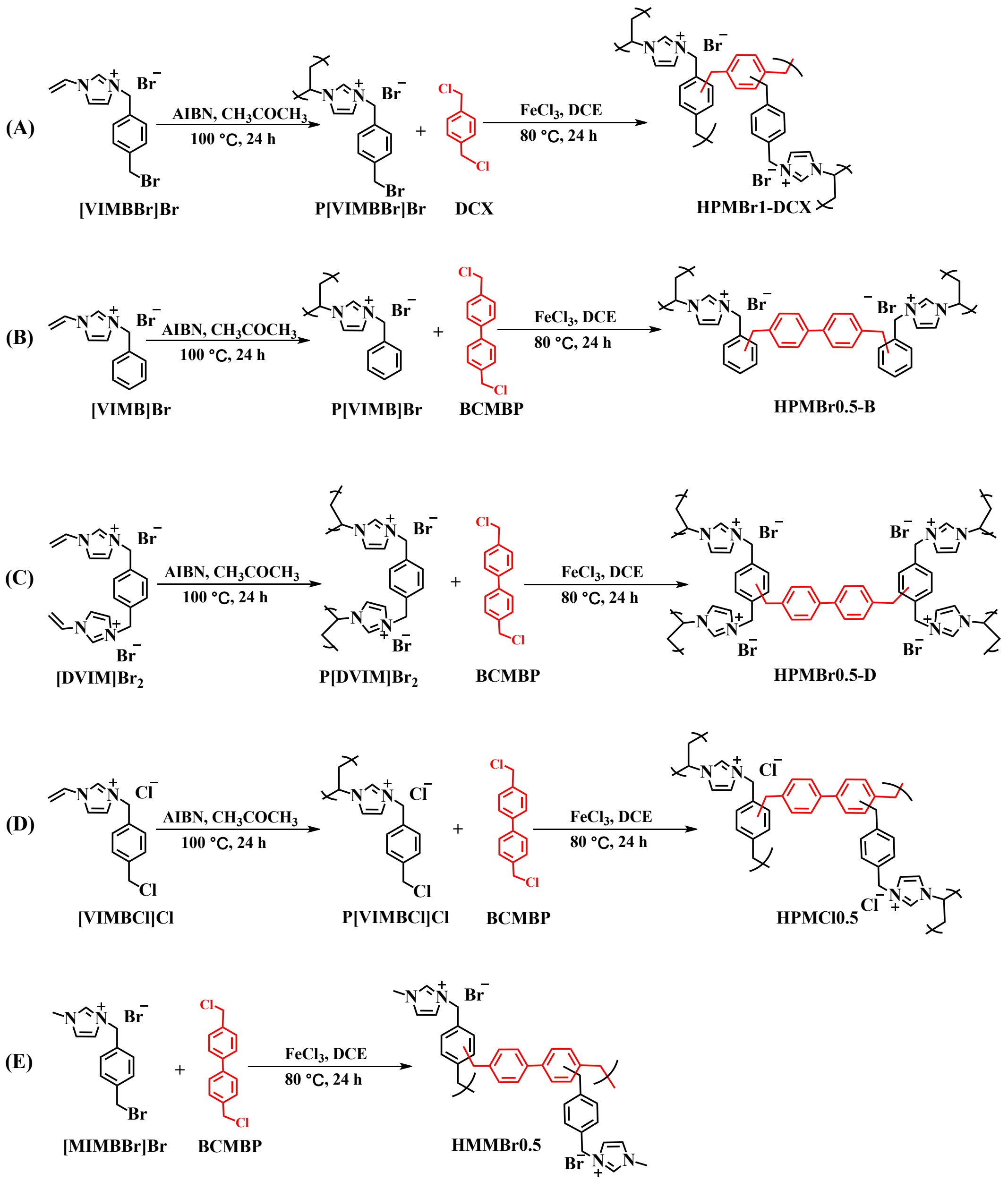

Scheme S6. Synthetic route to (A) HPMBr1-DCX, (B) HPMBr0.5-B, (C) HPMBr0.5-D, (D) HPMCl0.5 and (E) HMMBr0.5.

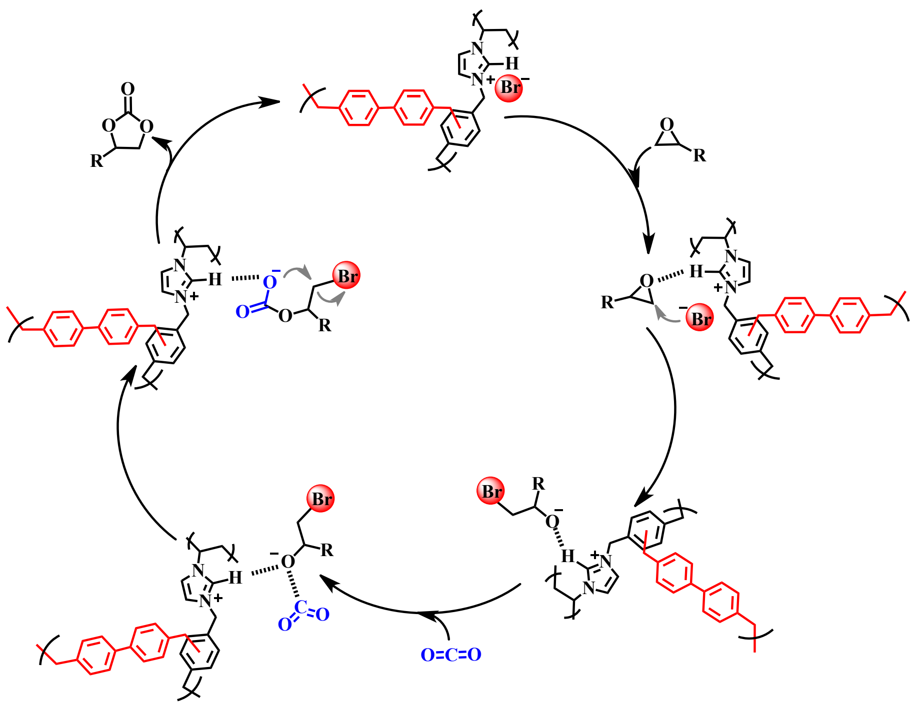

Scheme S7. Possible catalytic mechanism of CO_2 cycloaddition reaction over HPMBr0.5.

(A)

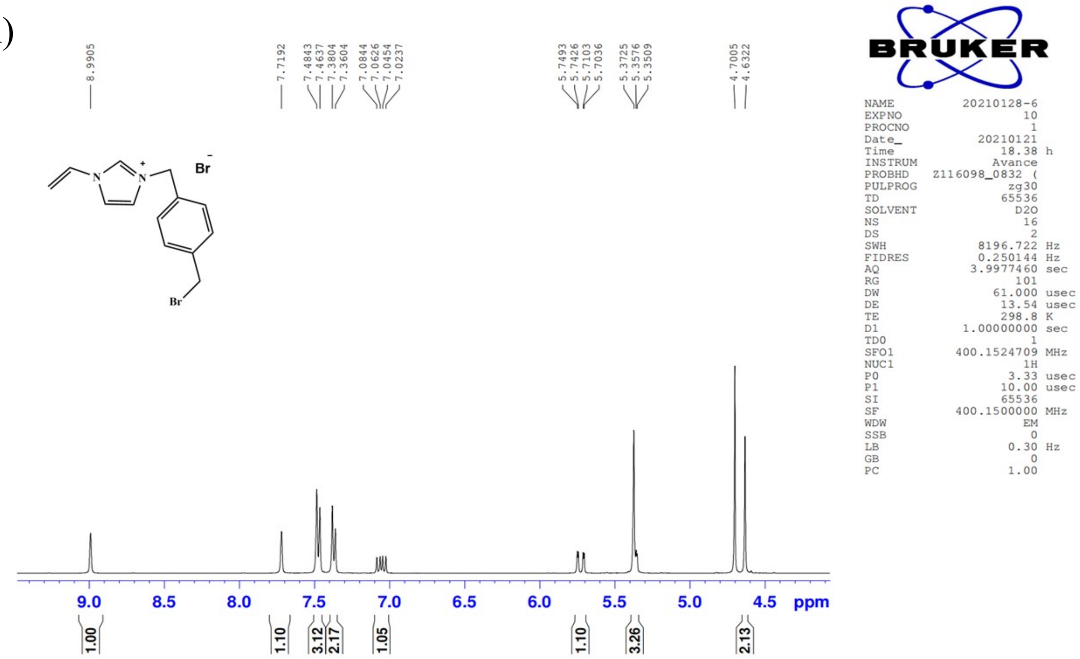

(B)

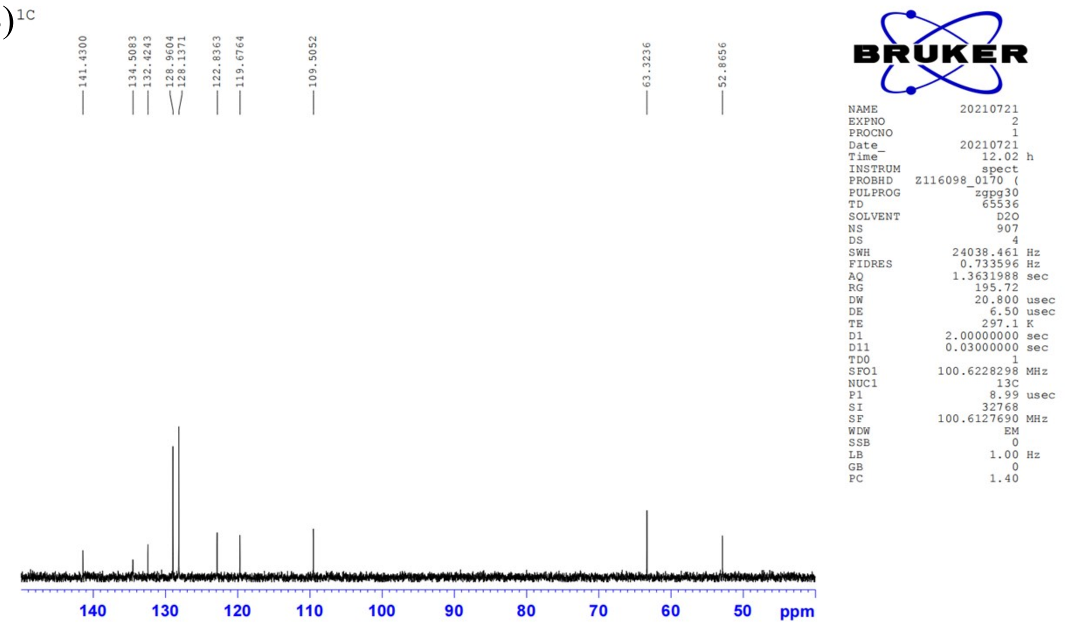

Figure S1. (A) ^{1}H NMR and (B) ^{13}C NMR of [VIMBBr]Br using D_2O as the solvent.

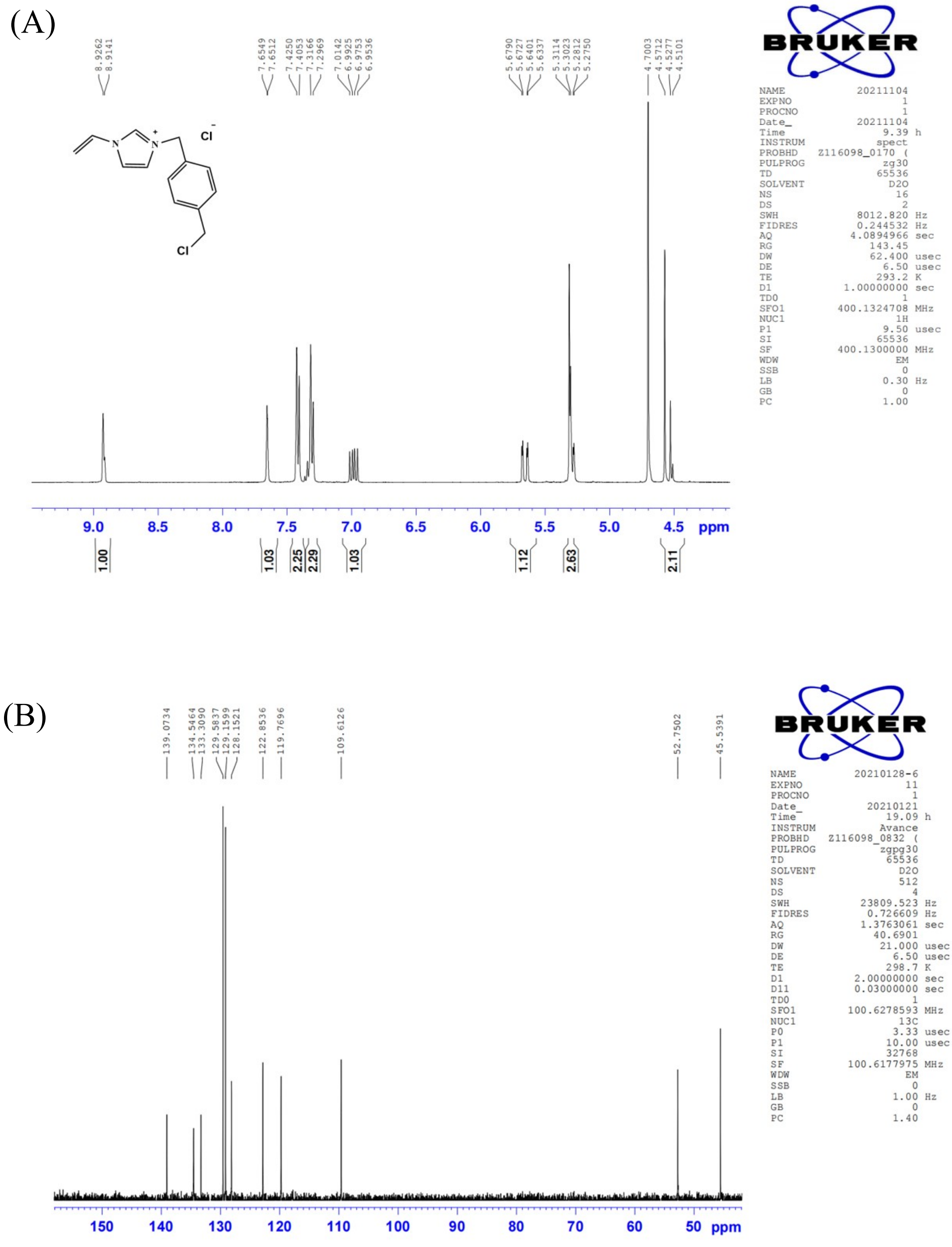

Figure S2. (A) ^{1}H NMR and (B) ^{13}C NMR of [VIMBCl]Cl using D_2O as the solvent.

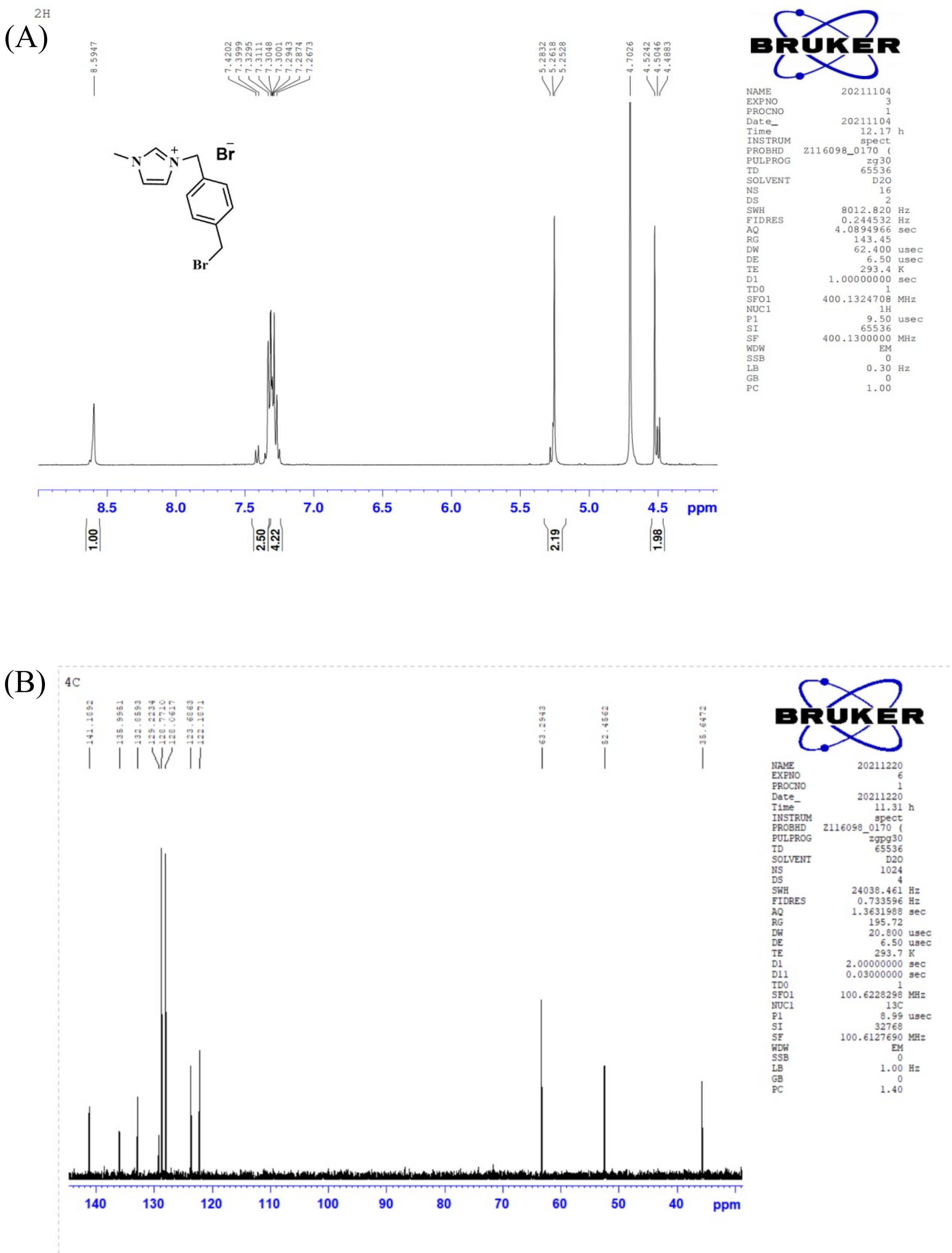

Figure S3. (A) ^{1}H NMR and (B) ^{13}C NMR of [MIMBBr]Br using D_2O as the solvent.

(A)

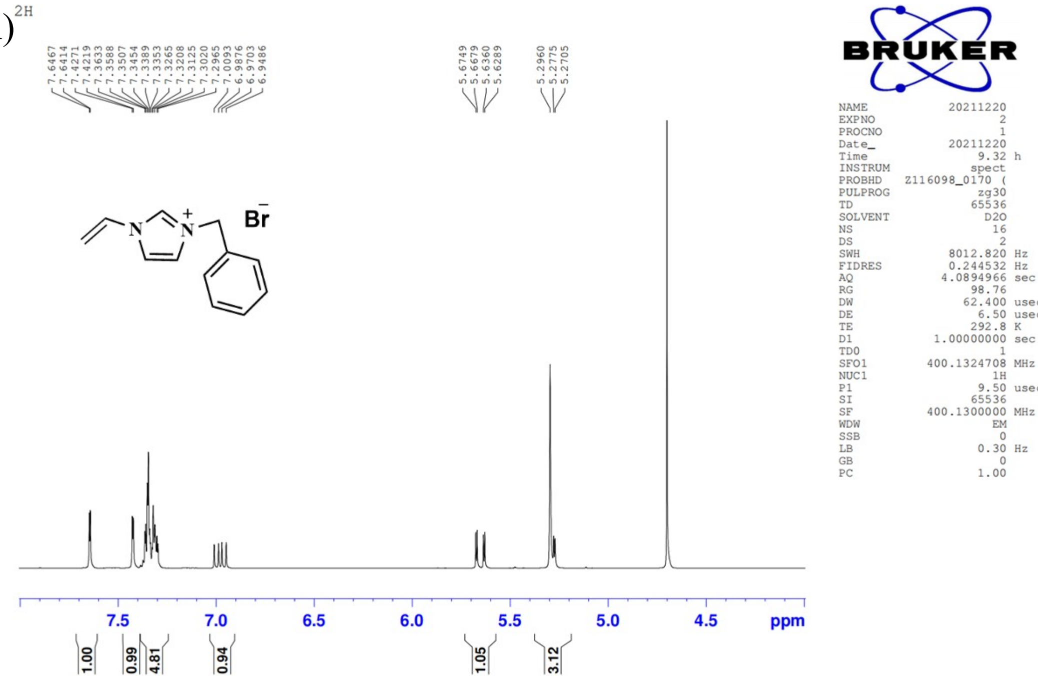

(B)

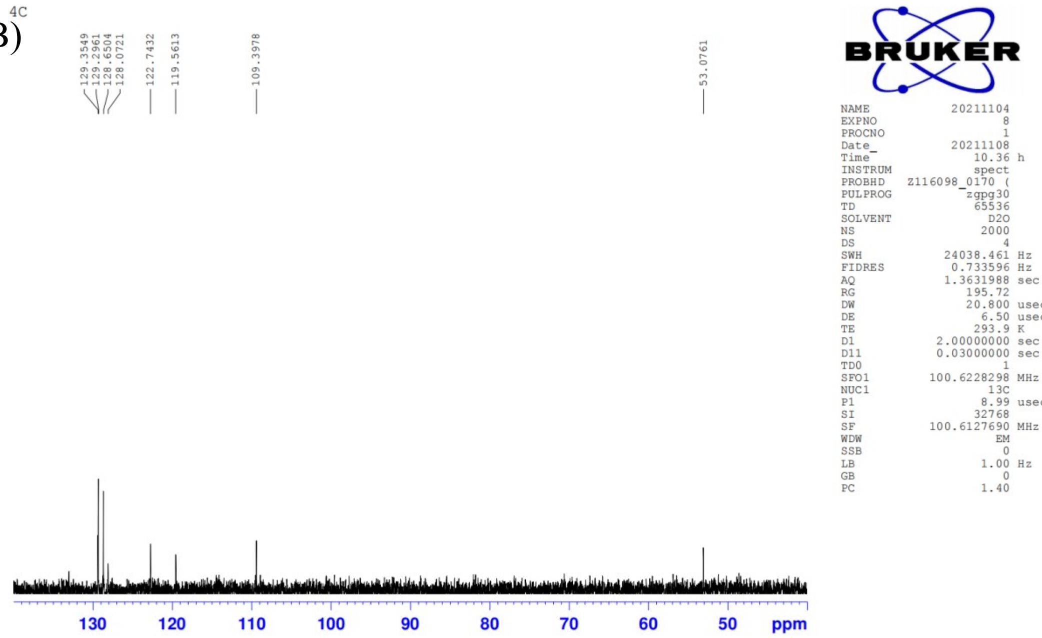

Figure S4. (A) ^{1}H NMR and (B) ^{13}C NMR of [VIMB]Br using D_2O as the solvent.

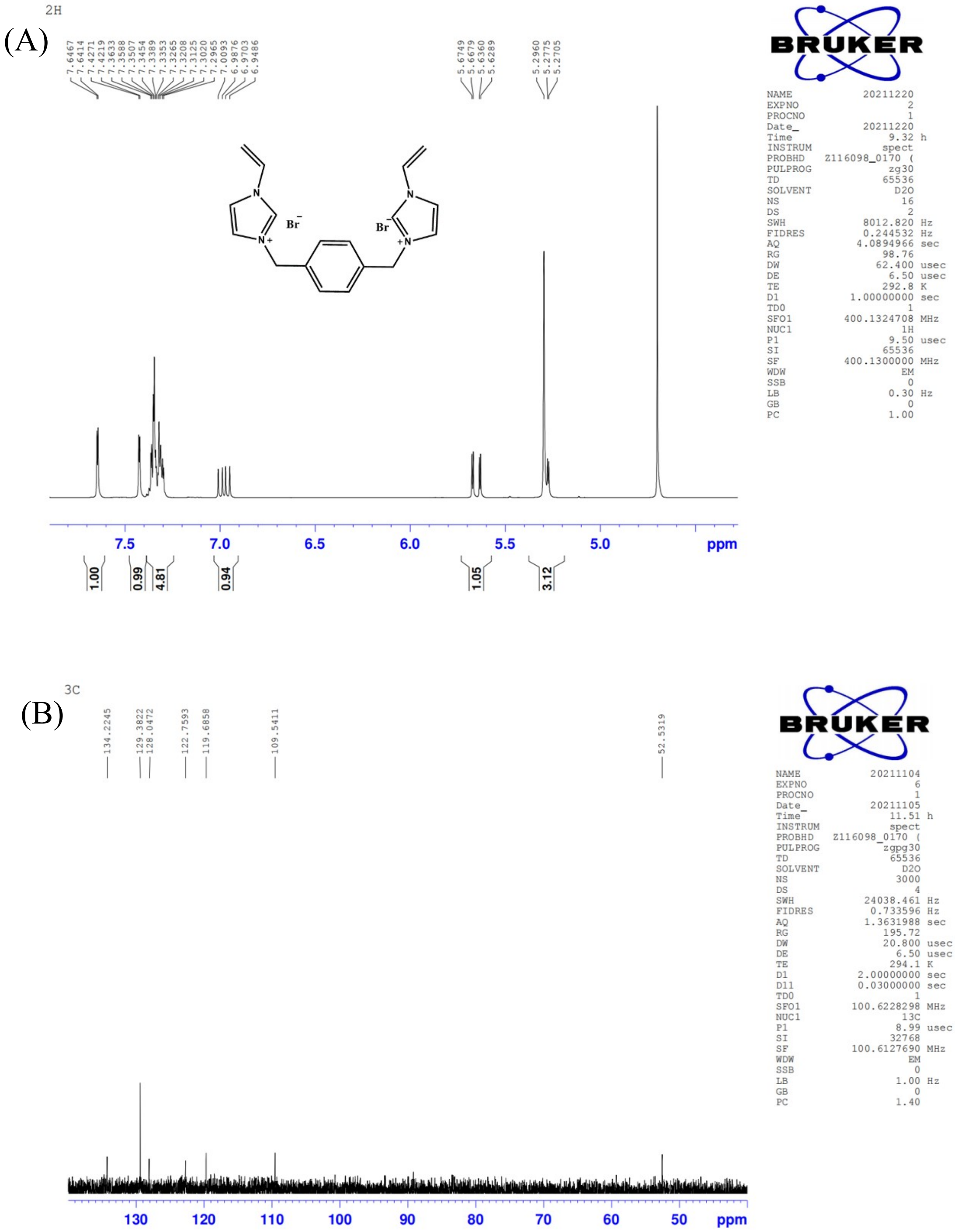

Figure S5. (A) ^{1}H NMR and (B) ^{13}C NMR of $[DVIMB]Br_2$ using D_2O as the solvent.

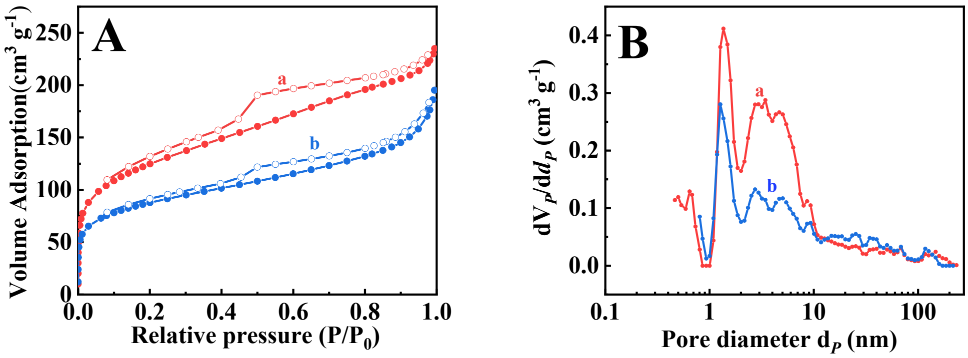

Figure S6. (A) Nitrogen sorption isotherms and (B) pore size distribution curves of HPMBr0.5 prepared with the molar composition of a) P[VIMBBr]Br/$FeCl_3$/BCMBP=1:2:0.5 and b) [VIMBBr]Br/$FeCl_3$/BCMBP=1: 8: 0.5.

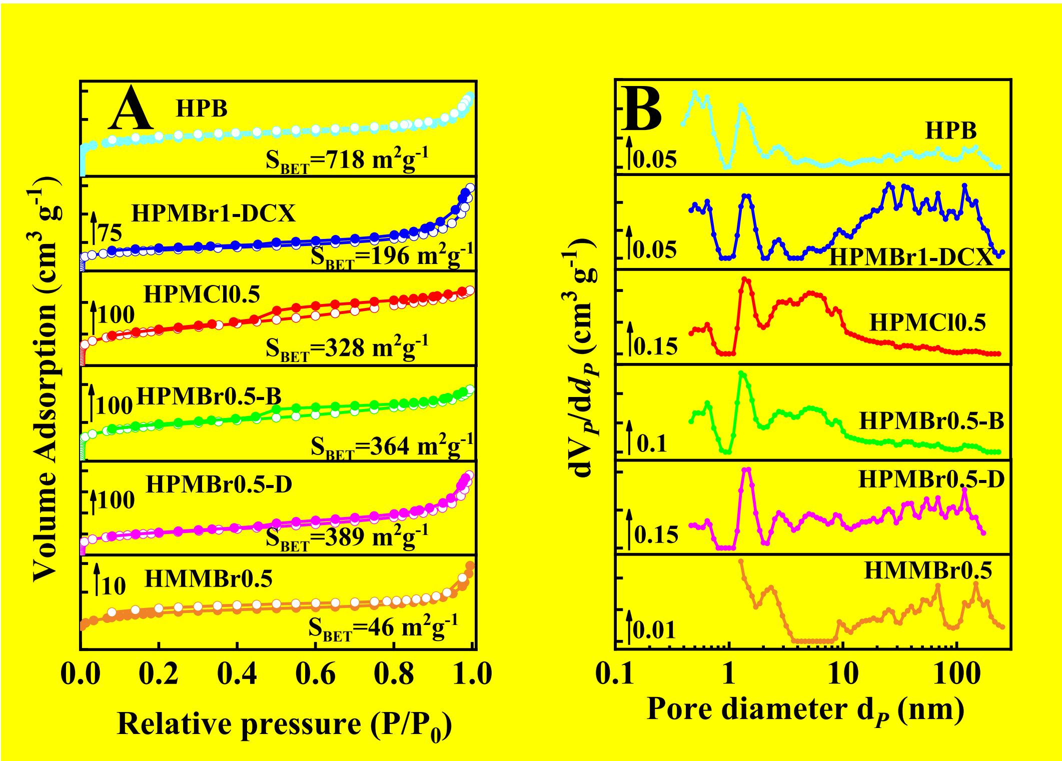

Figure S7. (A) Nitrogen sorption isotherms and (B) pore size distribution curves of HPB, H PMBr1-DCX, HPMCl0.5, HPMBr0.5-B, HPMBr0.5-D and HMMBr0.5.

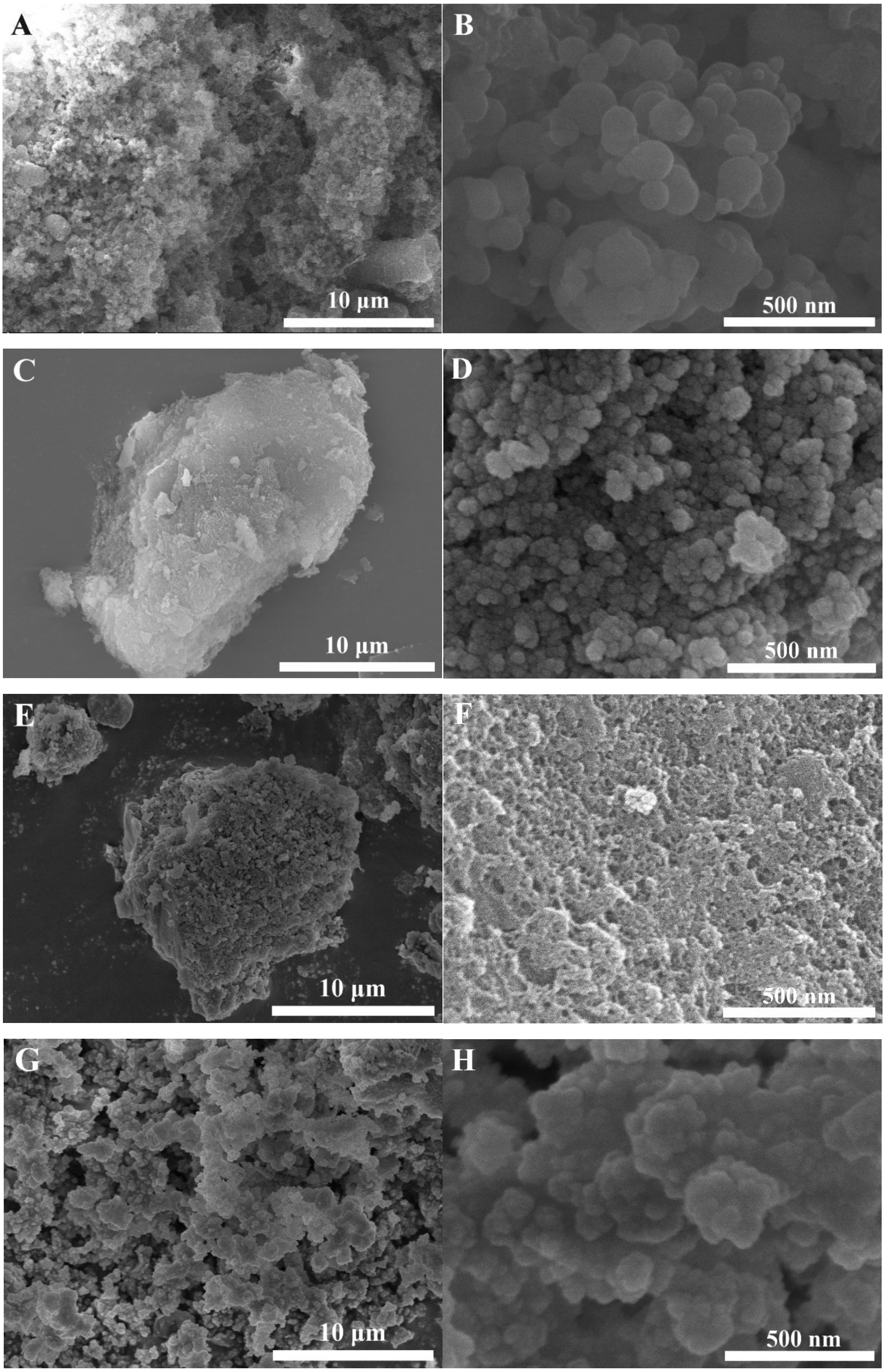

Figure S8. SEM images of (A, B) HPMBr0, (C, D) HPMBr0.3, (E, F) HPMBr0.75 and (G, H). HPB.

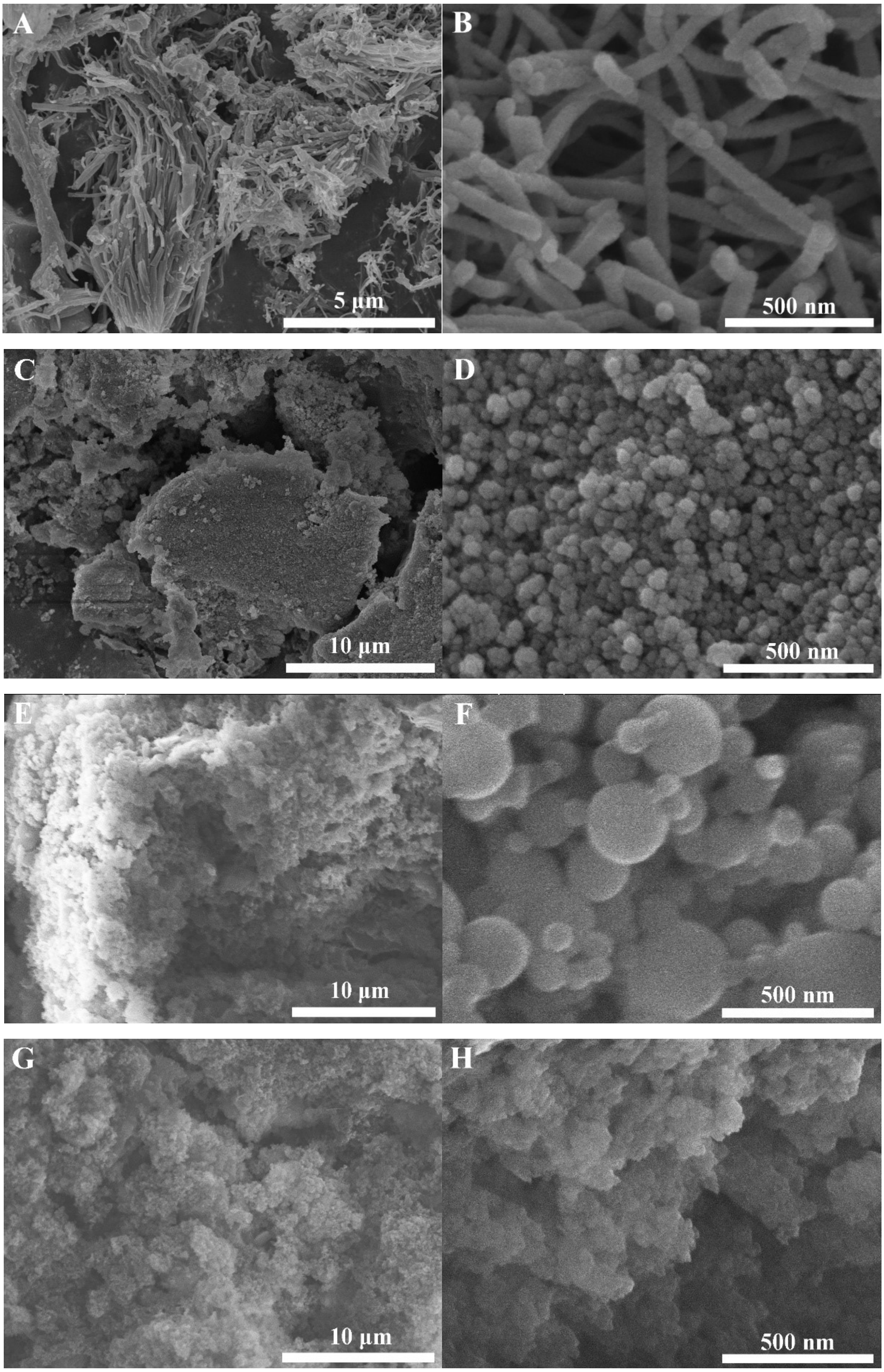
A
5 μm
B
500 nm
C
10 μm
D
500 nm
E
10 μm
F
500 nm
G
10 μm
H
500 nm

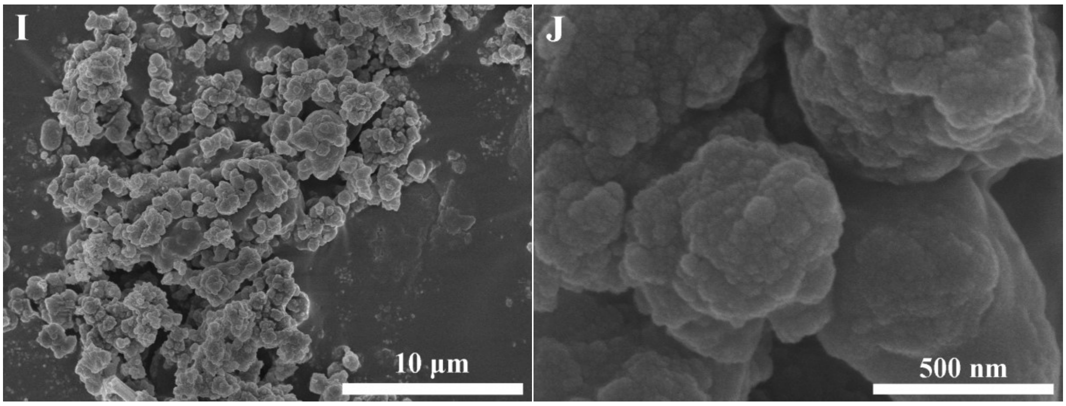

Figure S9. SEM images of (A, B) HPMCl0.5, (C, D) HPMBr1-DCX, (E, F) HPMBr0.5-B, (G, H) HPMBr0.5-D and (I, J) HMMBr0.5.

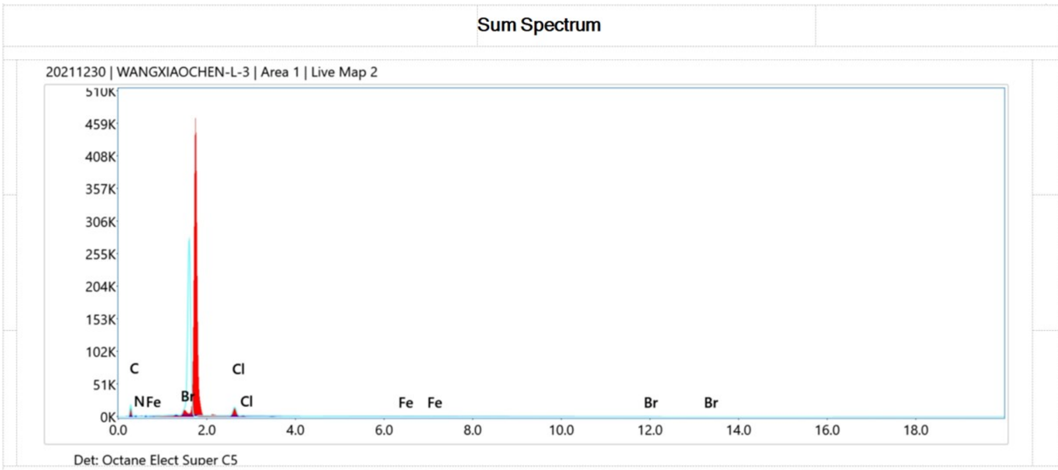

Figure S10. EDS spectrum of HPMBr0.5.

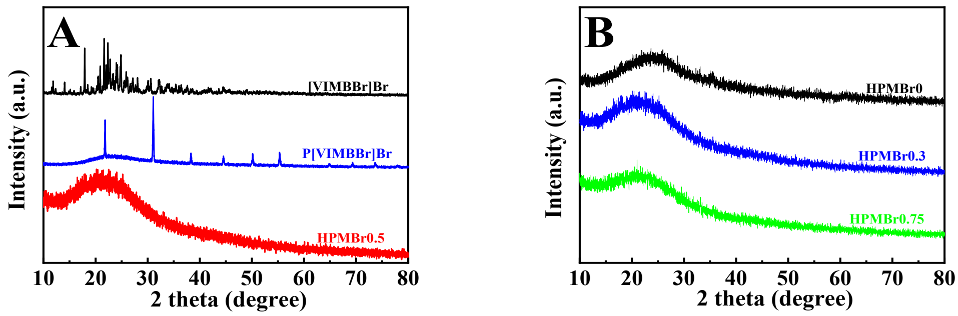

Figure S11. XRD patterns of [VIMBBr]Br, P[VIMBBr]Br and HPMBr*x*.

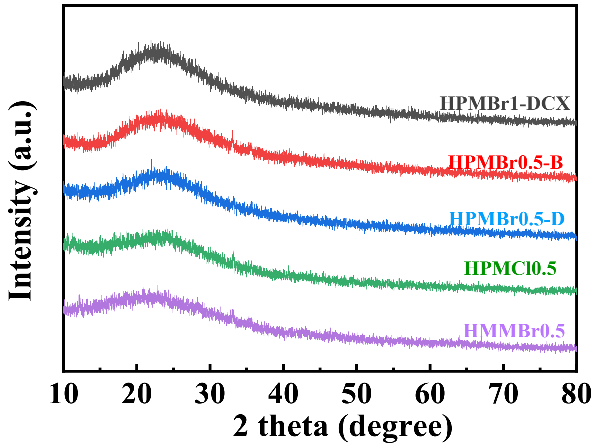

Figure S12. XRD patterns of HPMBr1-DCX, HPMBr0.5-B, HPMBr0.5-D, HPMCl0.5 and HMMBr0.5.

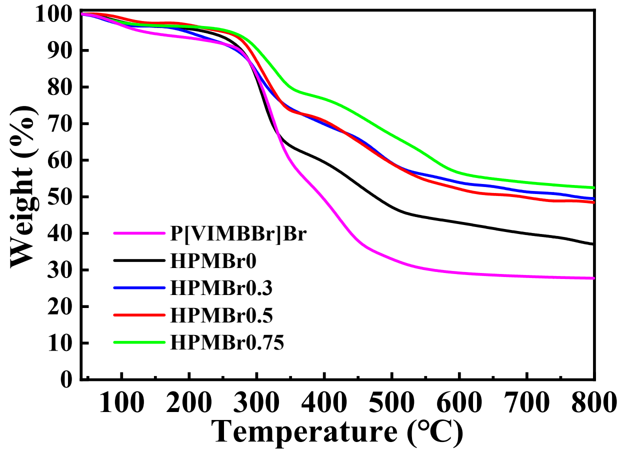

Figure S13. Thermogravimetry curves of P[VIMBBr]Br and HPMBr*x*.

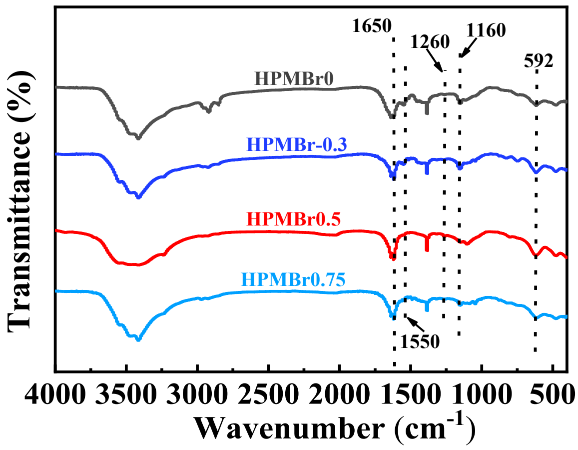

Figure S14. FT-IR spectra of HPMBr*x*.

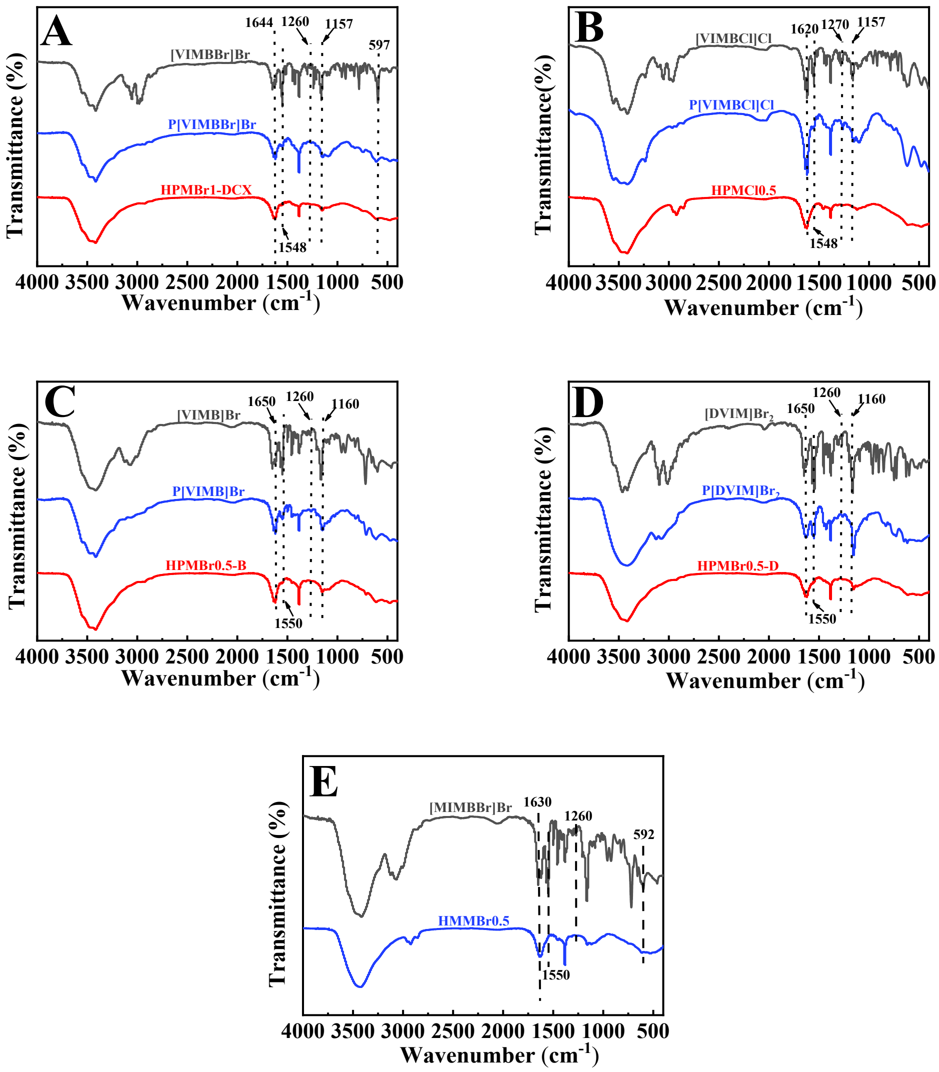

Figure S15. FT-IR spectra of control samples, corresponding IL monomers and linear precursors: (A) HPMBr1-DCX, (B) HPMCl0.5, (C) HPMBr0.5-B, (D) HPMBr0.5-D and (E) HMMBr0.5.

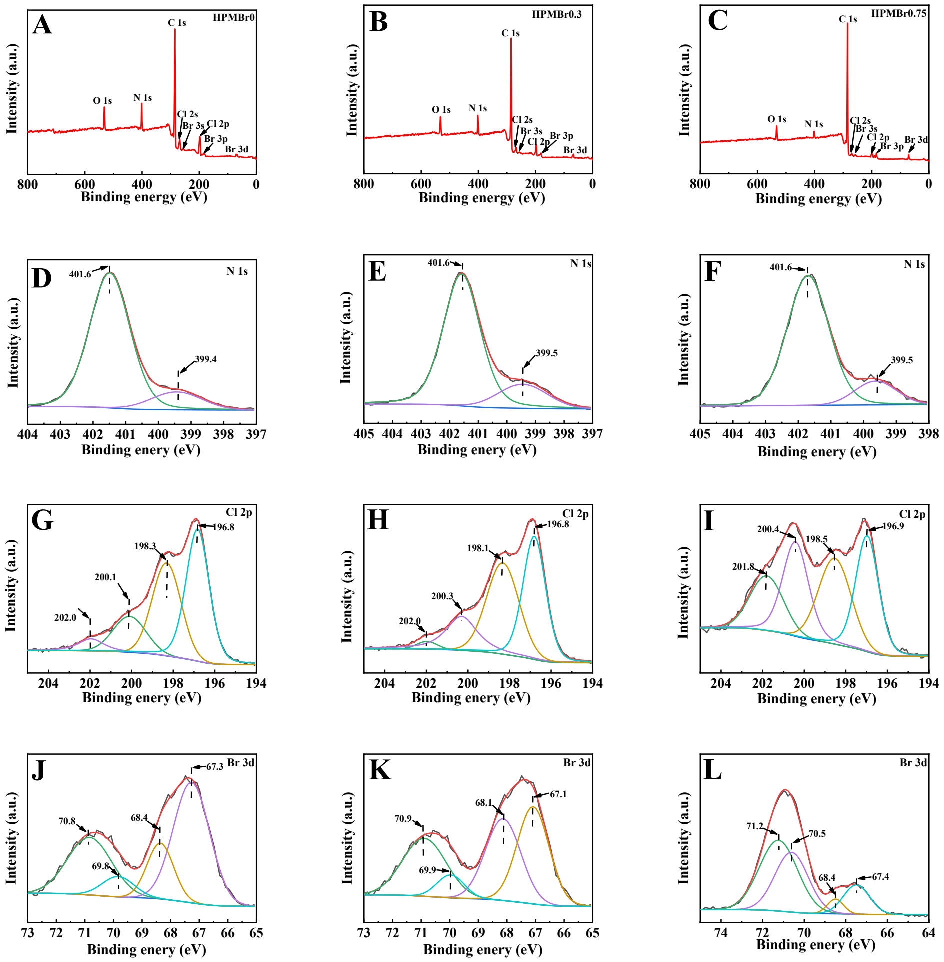

Figure S16. (A-C) XPS survey scan spectra, (D-F) N 1s, (G-I) Cl 2p and (J-L) Br 3d XPS spectra of HPMBr0, HPMBr0.3 and HPMBr0.75, respectively.

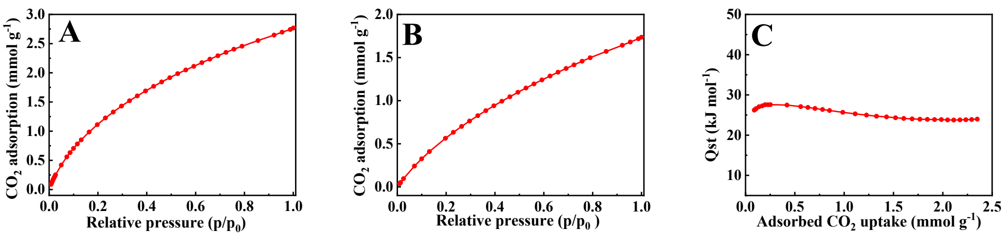

Figure S17. CO_2 sorption isotherms of HPB at (A)273 K and (B) 298 K; (C) the CO_2 isosteric heat of adsorption (Q_{st}) for HPB.

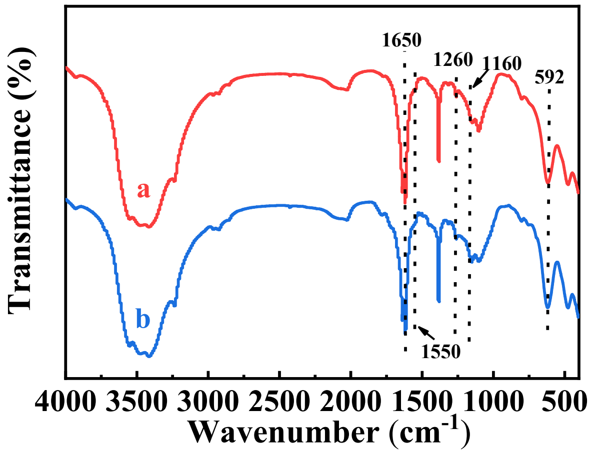

Figure S18. FT-IR spectra of a) fresh HPMBr0.5 and b) recovered HPMBr0.5 after 5th run.

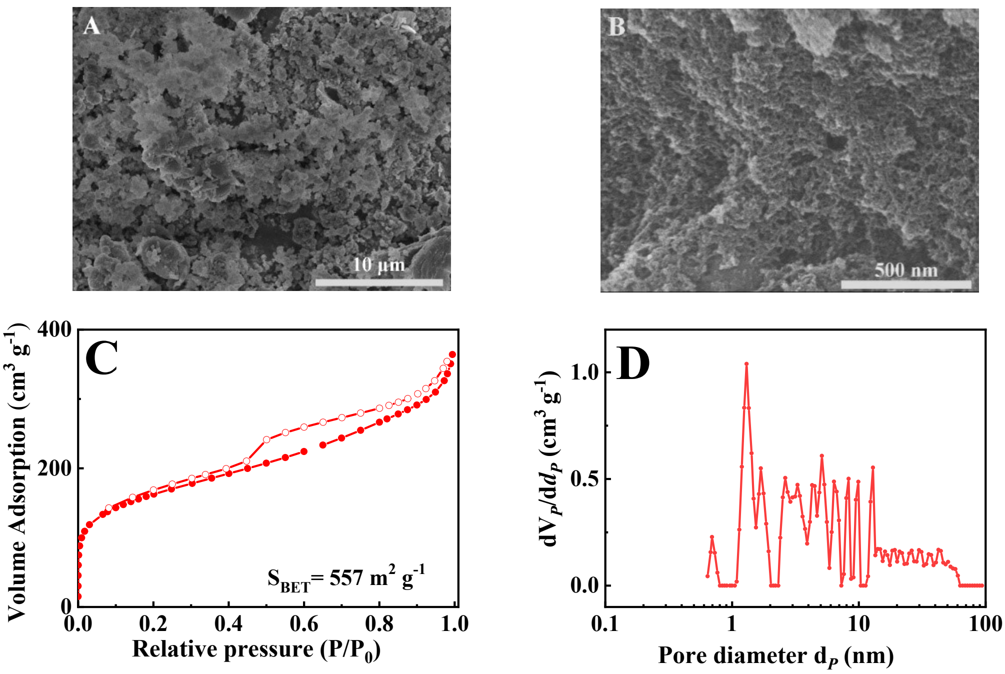

Figure S19. (A, B) SEM images, (C) N_2 sorption isotherm and (D) pore size distributions of recovered HPMBr0.5 after 5th run.

Table S1. Elemental analysis and synthetic yields for different samples.

Sample	N [%]	C [%]	H [%]	C/N ratio	C/H ratio	Yield[a] (%)
[VIMBBr]Br	7.92	43.71	3.54	5.52	12.35	---
P[VIMBBr]Br	8.48	51.16	4.16	6.03	12.30	98
HPMBr0	8.15	51.14	5.72	6.27	8.94	56
HPMBr0.3	6.85	57.16	5.16	8.34	11.07	80
HPMBr0.5	6.46	64.32	5.59	9.95	11.49	88
HPMBr0.75	6.14	63.61	5.10	10.35	12.48	94
HPMBr1-DCX	5.95	62.73	5.03	10.54	12.47	74
HPMBr0.5-B	4.81	63.56	5.17	13.21	12.29	68
HPMBr0.5-D	8.72	52.25	4.72	5.99	11.07	70
HPMCl0.5	5.90	62.98	5.11	10.67	12.32	88
HMMBr0.5	5.00	68.98	5.15	13.79	13.39	63
Reused HPMBr0.5	6.11	59.43	4.78	9.73	12.43	---

[a] The yield of polymer product.

Table S2. Textural properties of HPMBr0.5 prepared with the different molar composition of P[VIMBBr]Br, $FeCl_3$ and BCMBP.

Entry	**P[VIMBBr]Br /$FeCl_3$/BCMBP[a]**	**S_{BET}[b] (m^2 g^{-1})**	**S_{micro}[c] (m^2 g^{-1})**	**V_{total}[d] (cm^3 g^{-1})**	**V_{micro}[c] (cm^3 g^{-1})**	**Micropore content[e] (%)**	**D_{ave}[f] (nm)**
1	1/2/0.5	437.78	83.49	0.28	0.04	14	3.32
2	1/8/0.5	311.92	99.45	0.23	0.04	17	3.87

[a] The molar composition of P[VIMBBr]Br, $FeCl_3$ and BCMBP. [b] BET surface area. [c] Micropore surface area and volume calculated by the t-plot method. [d] Total pore volume. [e] Calculated by V_{micro}/V_{total}. [f] Average pore size.

Table S3. Comparison of various poly(ionic liquid)s between the surface area and IL content.

Entry	Sample	S_{BET} (m^2 g^{-1})	IL content (mmol g^{-1})	Synthesis approach	Ref.
1	**HPMBr0.5**	**558**	**2.31**	**FCA[c]**	**This**
2	**HPMBr0.75**	**855**	**2.19**	**FCA**	**This**
3	poly[bvbim]Cl	24.18	2.53[a]	FRP[d]	[1]
4	PDMBr	205	2.57[b]	FRP	[2]
5	$PIL_{1:1}$	86.21	2.21[a]	FRP	[3]
6	IP 3	91.56	1.69[b]	FRP	[4]
7	PQP	520	2.02[b]	FRP	[5]
8	PDBA-Cl-SCD	211	1.44[a]	FRP	[6]
9	PVIm-6-SCD	797.7	0.54[a]	FRP	[7]
10	PAD-3	156	2.32	FRP	[8]
11	[PAD][IDA]	132	1.72	FRP	[9]
12	PIL-4	1.97	1.25	FRP	[10]
13	AE-PIL-Cl	227.5	1.90	FRP	[11]
14	PGDBr-5-2OH	218	1.88	FRP	[12]
15	P-HVD-2/3/5	8.61	3.53	FRP	[13]
16	PADV-2	105	2.01	FRP	[14]
17	PDVB-[AlTMG]Br-0.2	152	1	FRP	[15]
18	POM3-IM	575	1.01[b]	FCA	[16]
19	Polymers 3	904	0.48[b]	FCA	[17]
20	Poly-NHC-2-Pd^{2+}	569	0.52	FCA	[18]
21	HCP-IL-7	447	0.70	FCA	[19]
22	HIP-Br-2	534	0.3	FCA	[20]
23	POPs-B10	824	0.81[b]	FCA	[21]
24	NHC-CAP-1(Zn^{2+})	1040	1.51	FCA	[22]
25	I_{C2}HCP-5b	1017	0.8	FCA	[23]
26	HCP-V2	750	0.50[b]	FCA	[24]
27	HPILs-Cl-2	500	1.24[b]	FCA	[25]
28	CPIP-A-4	570	0.53	FCA	[26]
29	IHCP-OH(1)	515	0.78	FCA	[27]
30	Bi/HCP_B	945.59	0.21[b]	FCA	[28]
31	Py-HCP-Br	435	0.76[b]	FCA	[29]
32	HP-[C4PhIm]Br-DCX-2	763	0.9	FCA	[30]
33	PiP@QA	301	1.89	FCA	[31]
34	DHI-CSU-3-Br	1216	1.21[b]	FCA	[32]
35	[HCP-CH2-Im][Cl]-1	385	2.10	FCA	[33]
36	PIP-3	1021.9	1.01	FCA	[34]
37	iPT-2	810	0.57	FCA	[35]
38	HIP-	323	0.81	FCA	[36]
39	HIP-Cl(3)-OH	596	0.97	FCA	[37]
40	iPHCP-12	537	0.98	FCA	[38]
41	IHCP-2	812	0.24[b]	FCA	[39]

[a] Estimated from their IL units. [b] Determined from CHN elemental analysis in reference. [c] Free-radical polymerization. [d] Friedel-Crafts alkylation.

Table S4. CO_2 adsorption performance of various polymers.

Entry	Sample	CO_2 uptake[a] (mmol g^{-1}) 273/298 K	Q_{st}[b] (KJ $mmol^{-1}$)
1	P[VIMBBr]Br	0.08/0.03	---[c]
2	HPMBr0	0.70/0.47	44
3	HPMBr0.3	0.87/0.52	53
4	HPMBr0.5	1.74/0.93	44
5	HPMBr0.75	1.83/0.94	38
6	HPB	2.83/1.78	26
7	HPMBr1-DCX	1.36/0.84	42
8	HPMCl0.5	1.26/0.80	35
9	HPMBr0.5-B	1.16/0.63	43
10	HPMBr0.5-D	1.26/0.72	45
11	HMMBr0.5	1.40/0.79	46

[a] CO_2 uptakes at 273 K and 298 K (0.1MPa). [b] Calculated by the Clausius-Clapeyron equation. [c] Negligible.

Table S5. Catalytic performances of control samples for CO_2 cycloaddition with ECH.[a]

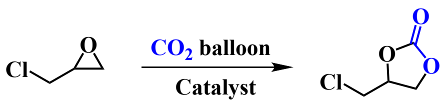

Entry	Sample	Con.[b] (%)	Sel.[c] (%)
1	HPB	0	0
2	HPMBr-DCX	81.8	96.5
3	HPMBr0.5-B	91.5	97.6
4	HPMBr0.5-D	84.3	96.9
5	HPMCl0.5	68.7	98.7
6	HMMBr0.5	96.3	98.9

[a] Reaction condition: catalyst (15 mg), ECH (5 mmol), 80 °C, 24 h, CO_2 (0.1MPa). [b] The conversion and selectivity determined by GC.

Table S6. Catalytic activity of recent metal-solvent-additive-free heterogeneous catalyst for cycloaddition of CO_2 under atmospheric pressure.

Entry	Catalyst	Epoxide	Temp. (°C)	Time (h)	Yield (%)	TOF[a] (h^{-1})	Ref.
1	**HPMBr0.5**	**ECH**	**80**	**24**	**99.0**	**6.0**	**This work**
2		**SO**	**80**	**36**	**94.7**	**3.8**	
3	PDMBr	ECH	70	48	91.3	0.73	[2]
4		SO	120	12	80.2	2.6	
5	IP 3	ECH	100	24	99	1.0	[4]
6		SO	100	24	87	0.9	
7	PDBA-Cl-SCD	ECH	90	6	99.4	3.4	[6]
8		SO	90	6	97.8	3.3	
9	PVIm-6-SCD	ECH	50	24	98.2	1.4	[7]
10		SO	80	18	97.9	1.4	
11	PAD-3	ECH	70	24	98	0.88	[8]
12		SO	110	8	92	2.4	
13	PGDBr-5-2OH	ECH	70	24	91	1.9	[12]
14		SO	70	96	90	0.49	
15	PADV-2	ECH	50	24	87	3.8	[14]
16		SO	90	24	96	3.4	
17	[HCP-CH2-Im][Cl]-1	ECH	140	4	99	2.6	[33]
18		SO	100	20	93	0.74	
19	HIP-Cl(3)-OH	SO	100	20	98	2.3	[37]
20	iPHCP-12	ECH	60	60	99	0.67	[38]
21		SO	80	60	95	0.64	
22	DB10%-Pa-Tp	ECH	120	96	99	4.4	[40]
23	COP-222	ECH	100	24	99	1.2	[41]
24		SO	100	24	99	1.2	
25	COF-IL	ECH	80	48	98	0.68	[42]
26		SO	80	48	98	0.68	
27	[PDVB-HAVIM-C_{18}]Br	ECH	80	16	96.4	4.3	[43]
28		SO	80	30	93.5	2.2	
29	IM-iPHP-2	ECH	80	48	96	1.4	[44]
30		SO	80	72	84	0.85	
31	VIPA-Br	SO	80	72	96	0.14	[45]

[a] Turnover frequency (TOF): yield of cyclic carbonate (mmol)/[ionic sites (mmol)×reaction time (h)]

Table S7. Dosage of catalyst and catalytic performance of HPMBr0.5 and previously reported hypercrosslinked poly(ionic liquid)s *via* preparation of Friedel-Crafts alkylation.

Entry	Catalyst	Epoxide	Dosage[a] (wt%)	Co-catalyst	P (MPa)	Temp. (°C)	Time (h)	Yield (%)	Ref.
1	**HPMBr0.5**	**ECH**	**3.2**	**None**	**0.1**	**80**	**24**	**99.0**	**This work**
					1.0	**80**	**6**	**99.3**	
2		**SO**	**2.5**	**None**	**0.1**	**80**	**36**	**94.7**	**This work**
					1.0	**80**	**6**	**97.5**	
3[b]	POM3-IM	ECH	53.8	None	1.0	120	8	90.0	[16]
4[c]	Polymers 3	ECH	11.4	$ZnBr_2$	1.0	130	7	91	[17]
5	HIP-Br-2	SO	5.4	None	1.0	120	6	99	[20]
6	HPILs-Cl-2	ECH	5.4	TBAB	0.1	70	9	99.0	[25]
7	IHCP-OH(1)	ECH	0.4	None	3.0	135	1	99.0	[27]
8	Py-HCP-Br	ECH	12.6	None	2.0	120	8	99.0	[29]
9	HP-[BZPhIm]Cl-DCX-1	SO	6.5	None	0.1	120	24	90.9	[30]
10	DHI-CSU-3-Br	ECH	10.8	TBAB	0.1	70	8	99.0	[32]
11	[HCP-CH2-Im][Cl]-1	SO	25	None	0.1	140	4	95	[33]
12	PIP-3	SO	4.2	None	1.0	100	24	98	[34]
13	HIP-Cl(3)-OH	SO	16.7	None	0.1	120	12	99	[37]
14	iPHCP-12	ECH	27.0	None	0.1	60	60	99	[38]

[a] Dosage of catalyst. [b] ethanol as solvent. [c] DMF as solvent.

Characterization of cyclic carbonates

4-methyl-1,3-dioxolan-2-one:

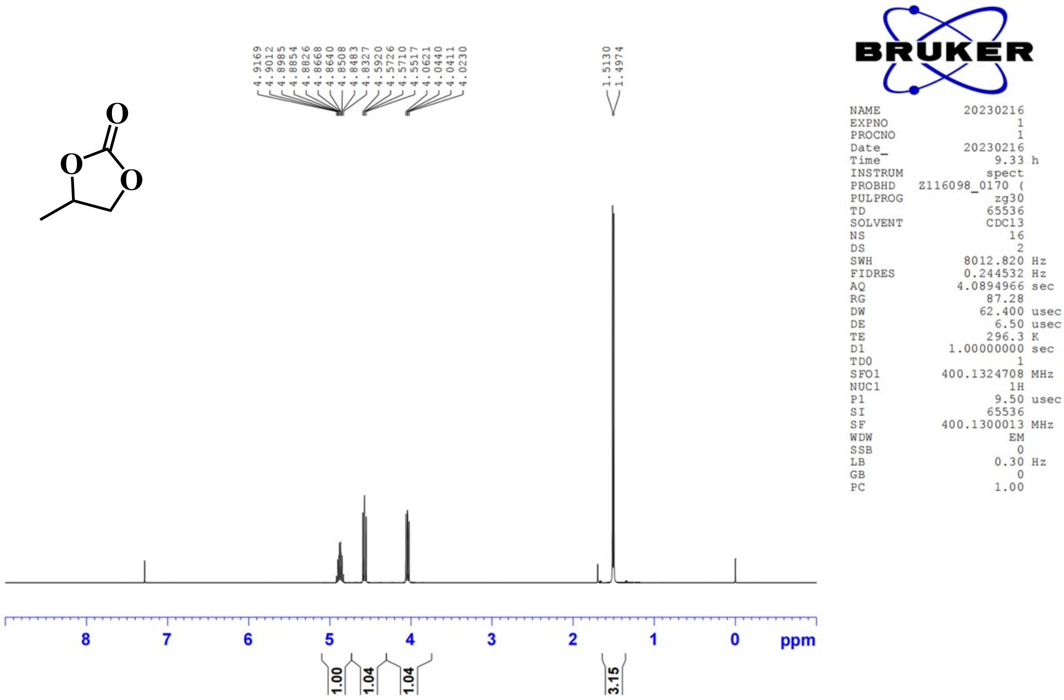

^{1}H NMR (400 MHz, $CDCl_3$): δ 4.91 (m, 1H), 4.58 (q, 1H), 4.05 (q, 1H), 1.50 (d, 3H).

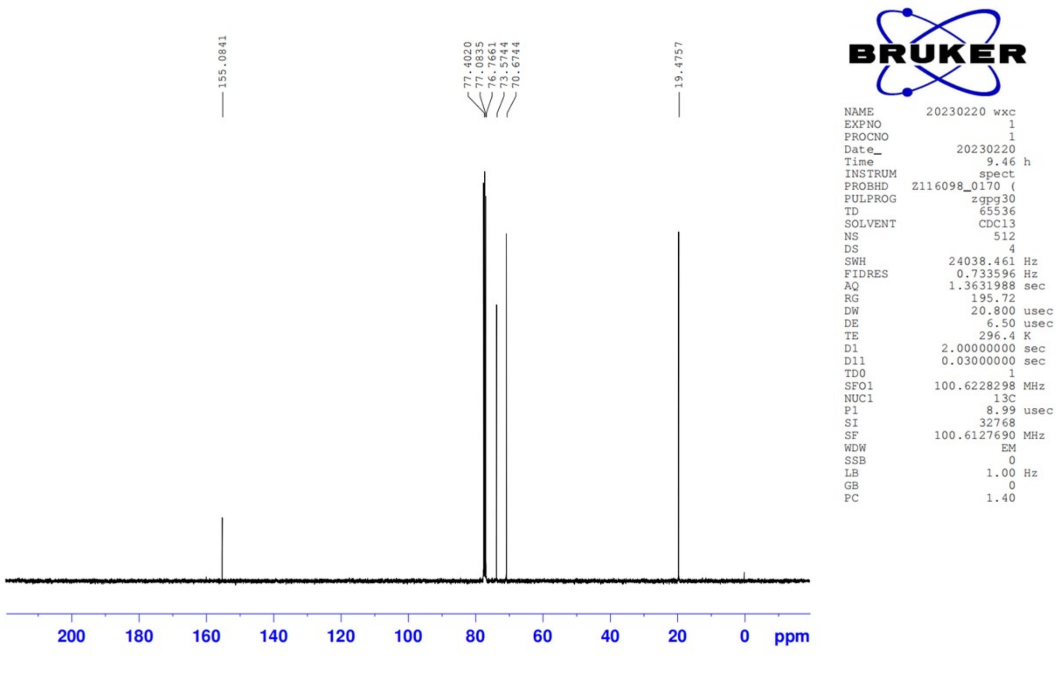

^{13}C NMR (100 MHz, $CDCl_3$): δ 155.1, 73.6, 70.7, 19.5.

4-(chloromethyl)-1,3-dioxolan-2-one:

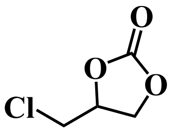

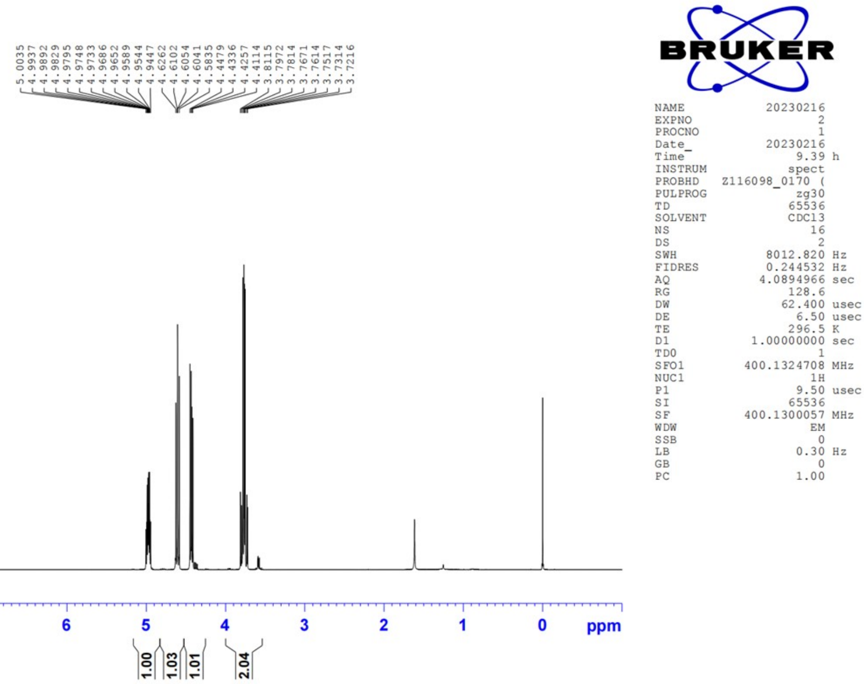

^1H NMR (400 MHz, $CDCl_3$): δ 5.00 (m, 1H), 4.63 (m, 1H), 4.45 (q, 1H), 3.81 (m, 2H).

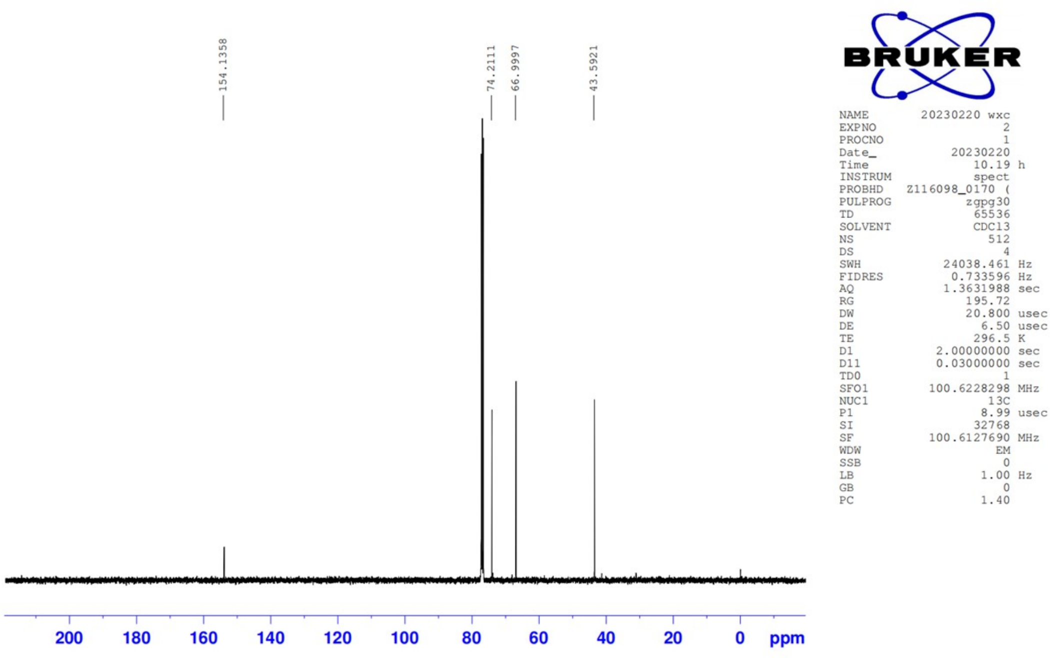

^{13}C NMR (100 MHz, $CDCl_3$): δ 154.1, 74.2, 67.0, 43.6.

4-phenyl-1,3-dioxolan-2-one:

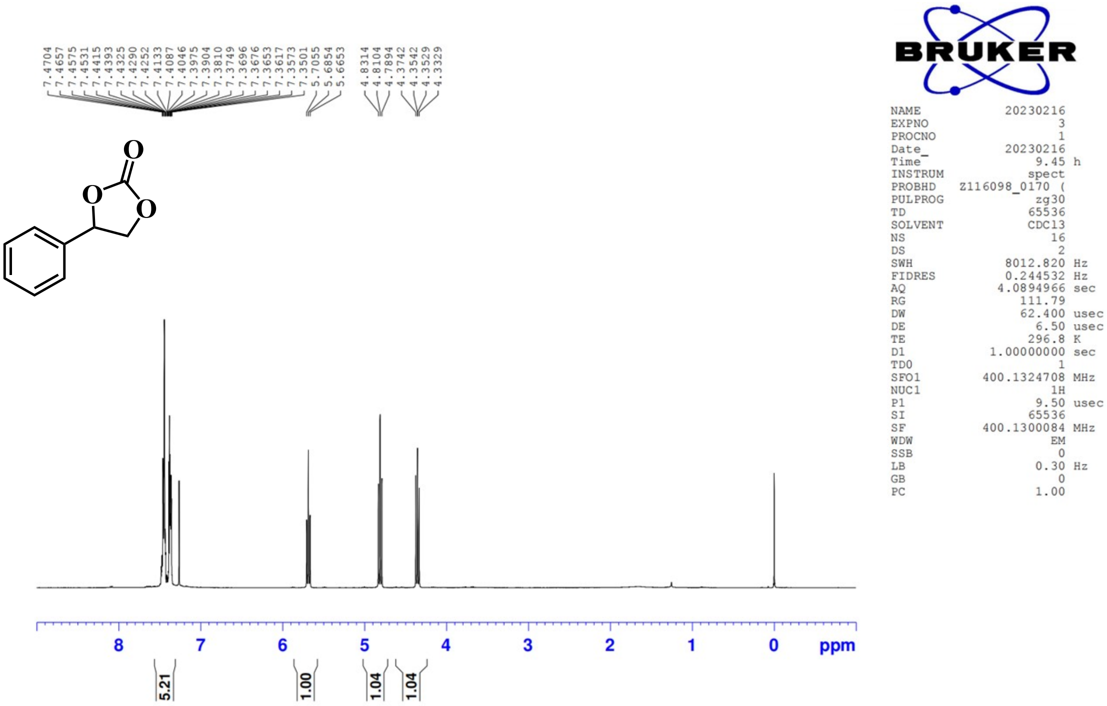

^{1}H NMR (400 MHz, $CDCl_3$): δ 7.44 (m, 5H), 5.70 (t, 1H), 4.83 (t, 1H), 4.37 (q, 1H).

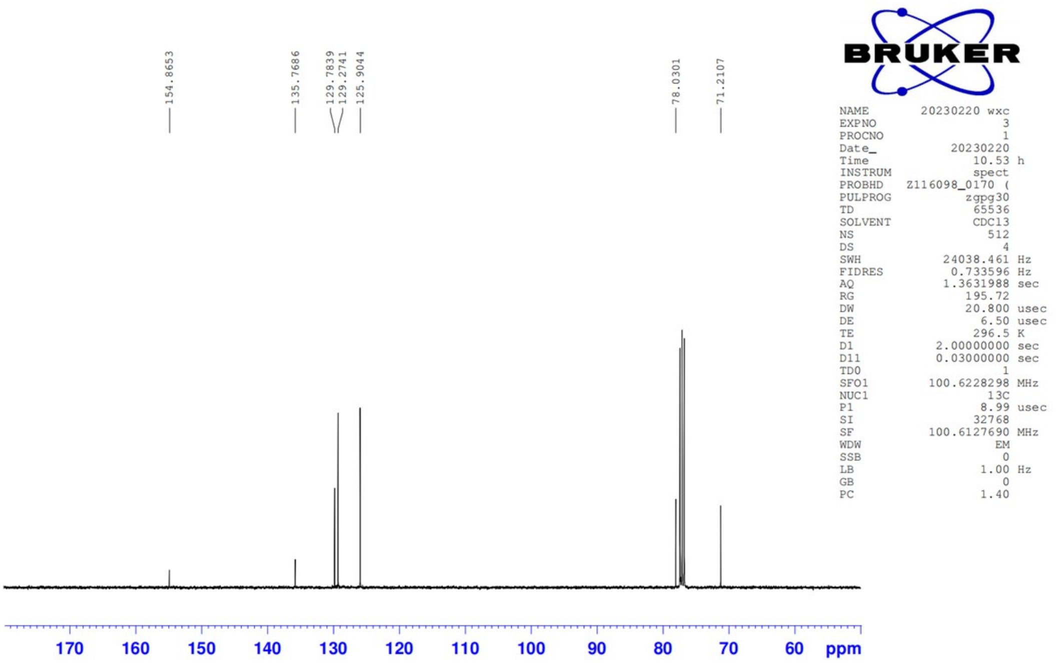

^{13}C NMR (100 MHz, $CDCl_3$): δ 154.9, 135.8, 129.8, 129.3, 125.9, 78.0, 71.2.

allyloxymethyl-1,3-dioxolan-2-one:

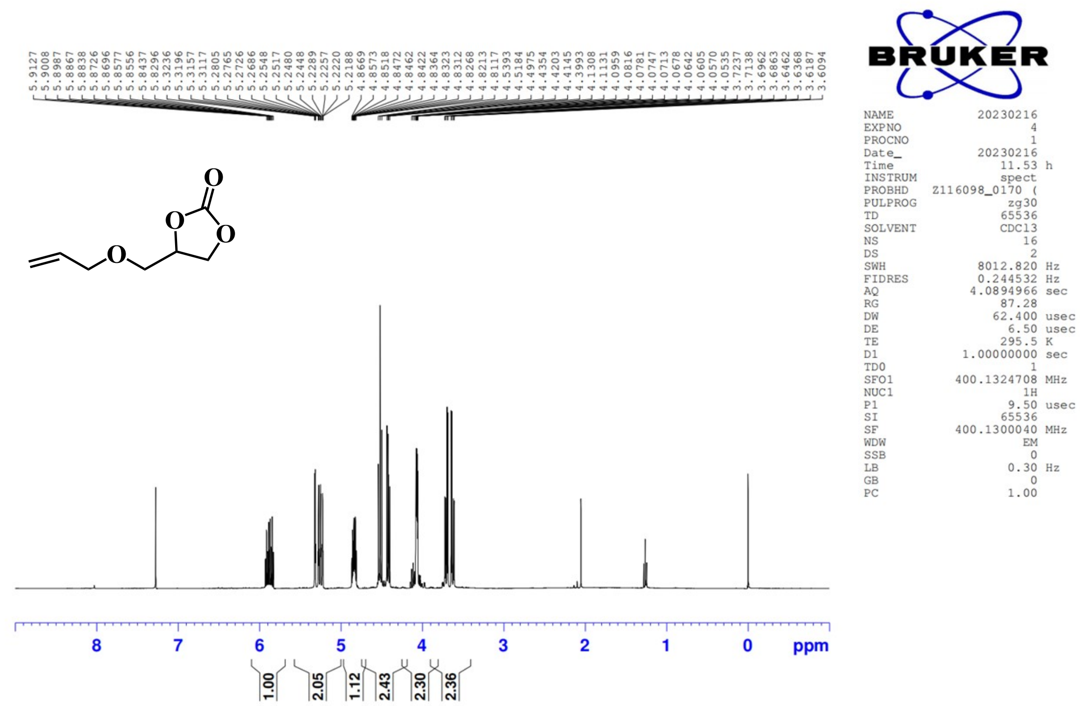

[1]H NMR (400 MHz, $CDCl_3$): δ 5.91 (m, 1H), 5.32-5.22 (m, 2H), 4.87 (m, 1H), 4.53 (t, 1H), 4.42 (q, 1H), 4.12 (m, 2H), 3.72 (m, 2H).

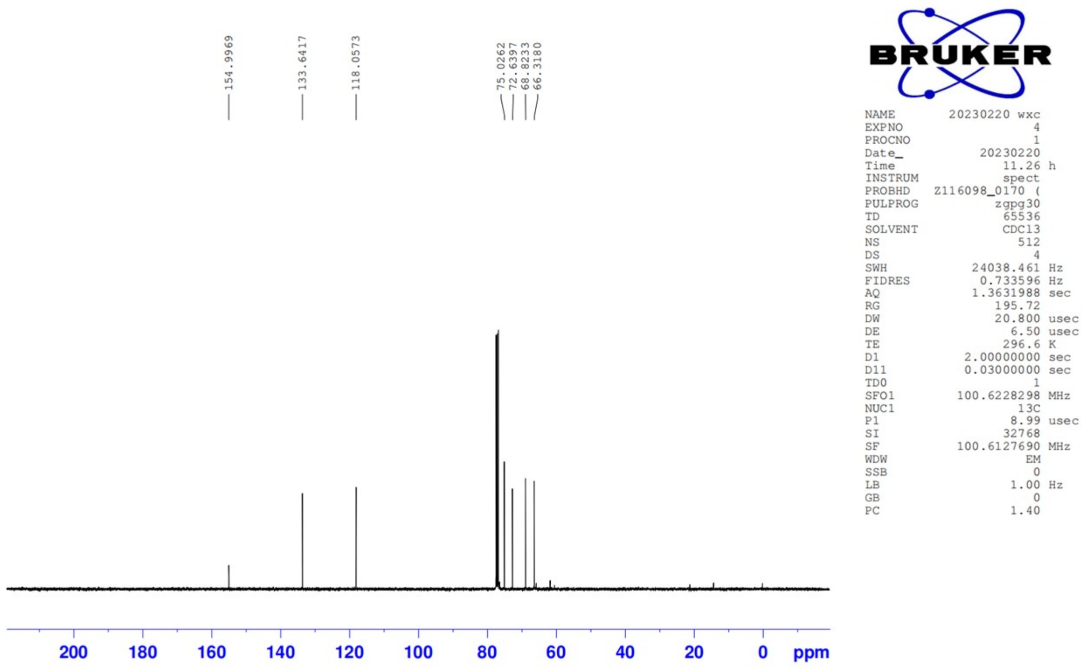

[13]C NMR (100 MHz, $CDCl_3$): δ 155.0, 133.6, 118.1, 75.0, 72.6, 68.8, 66.3.

4-(phenoxymethyl)-1,3-dioxolan-2-one:

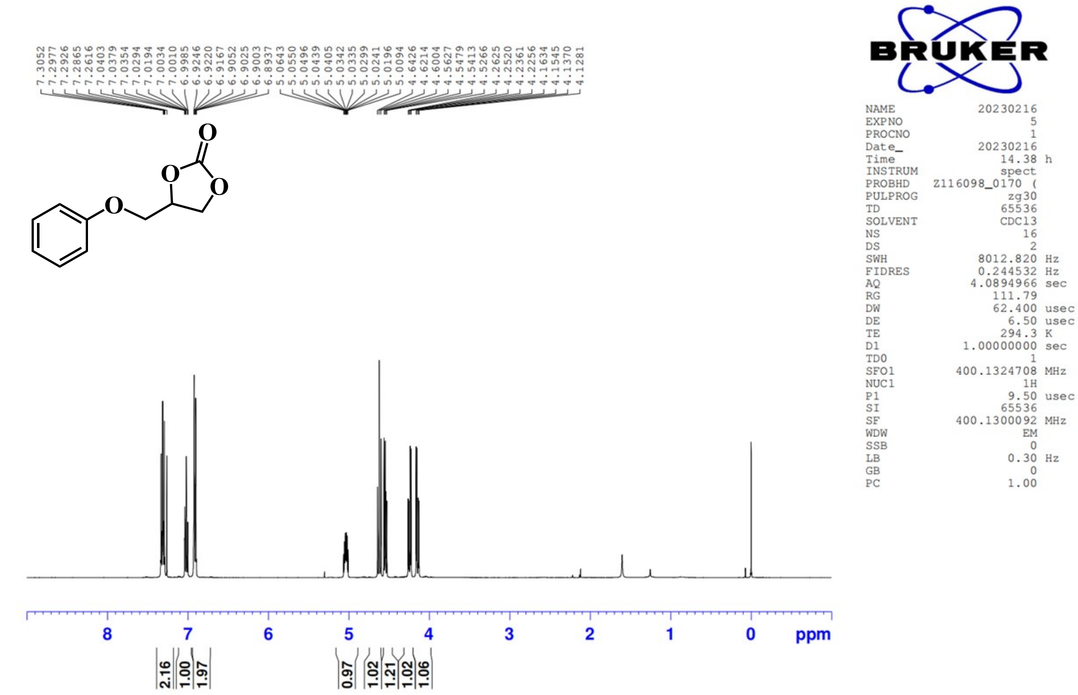

^{1}H NMR (400 MHz, $CDCl_3$): δ 7.31 (m, 2H), 7.03 (t, 1H), 6.92 (t, 2H,), 5.05 (m, 1H), 4.63 (t, 1H), 4.54 (q, 1H), 4.25 (q, 1H), 4.16 (q, 1H).

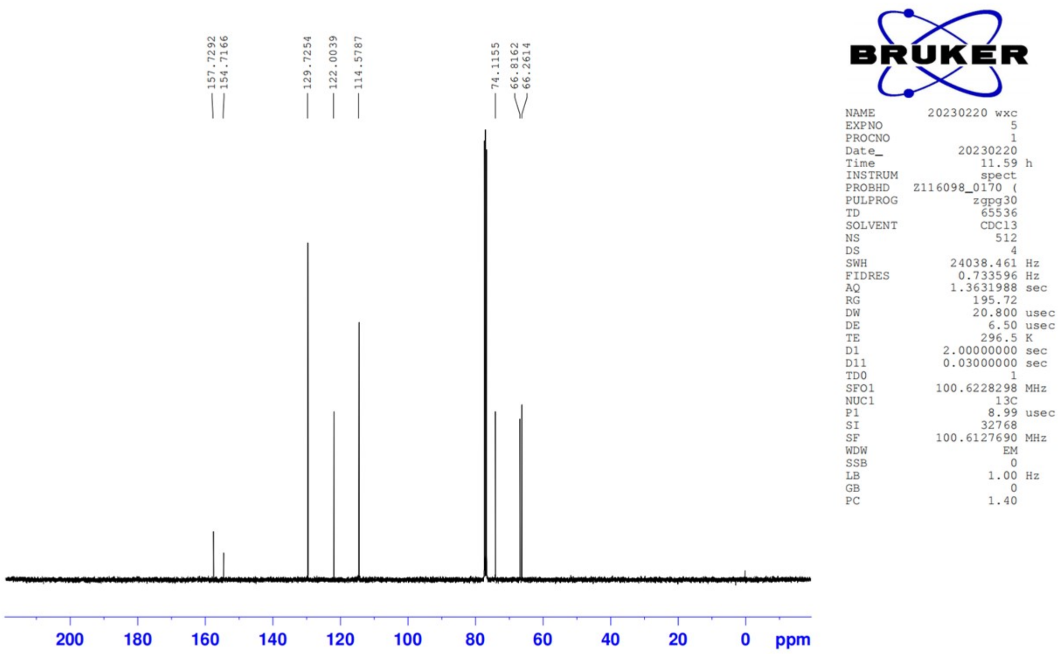

^{13}C NMR (100 MHz, $CDCl_3$): δ 157.8, 154.7, 129.7, 122.0, 114.6, 74.1, 66.9, 66.2.

4-butyl-1,3-dioxolan-2-one:

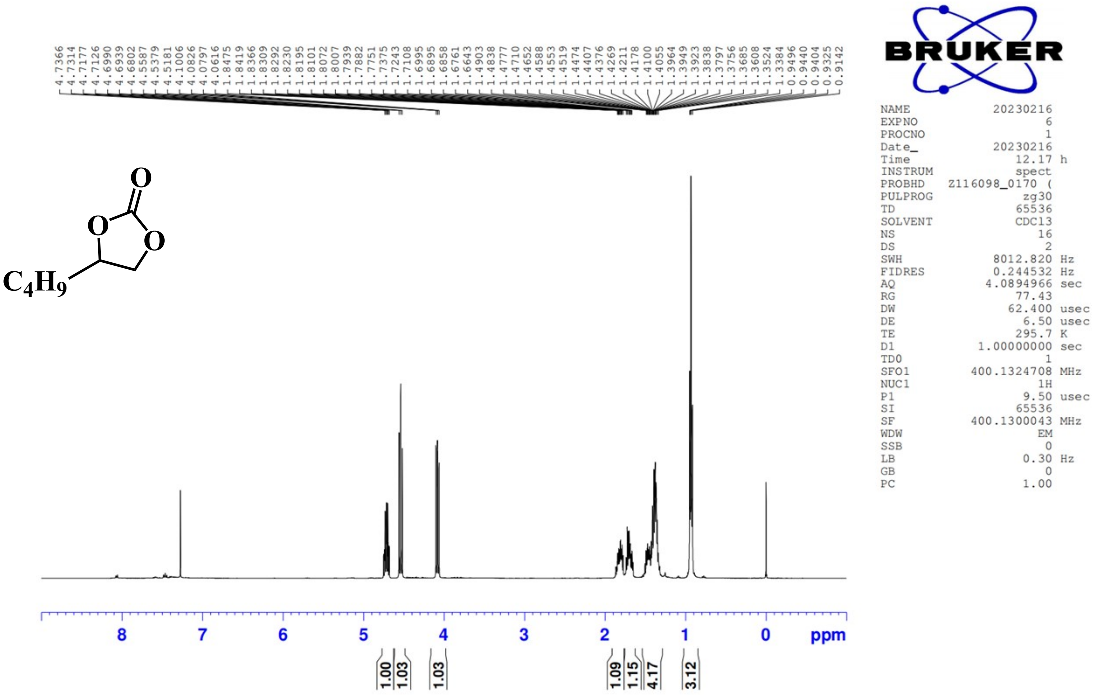

[1]H NMR (400 MHz, $CDCl_3$): δ 4.74 (m, 1H), 4.55 (t, 1H), 4.09 (q, 1H), 1.84 (m, 2H), 1. 49(m, 4H), 0.95 (t, 3H).

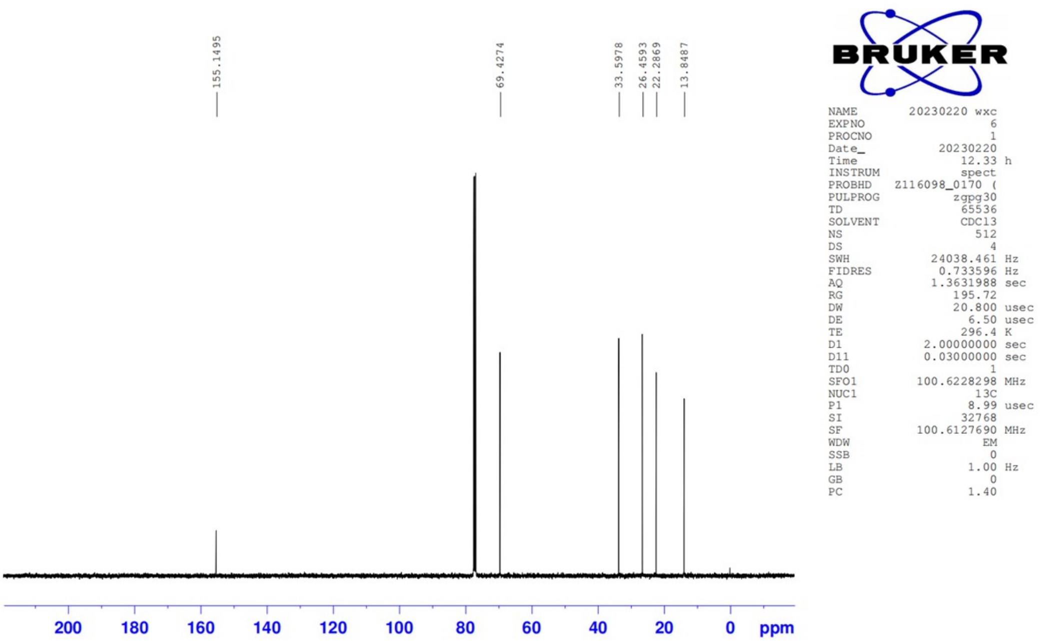

[13]C NMR (100 MHz, $CDCl_3$): δ 155.1, 77.1, 69.4, 33.5, 26.4, 22.2, 13.8.

4-octyl-1,3-dioxolan-2-one:

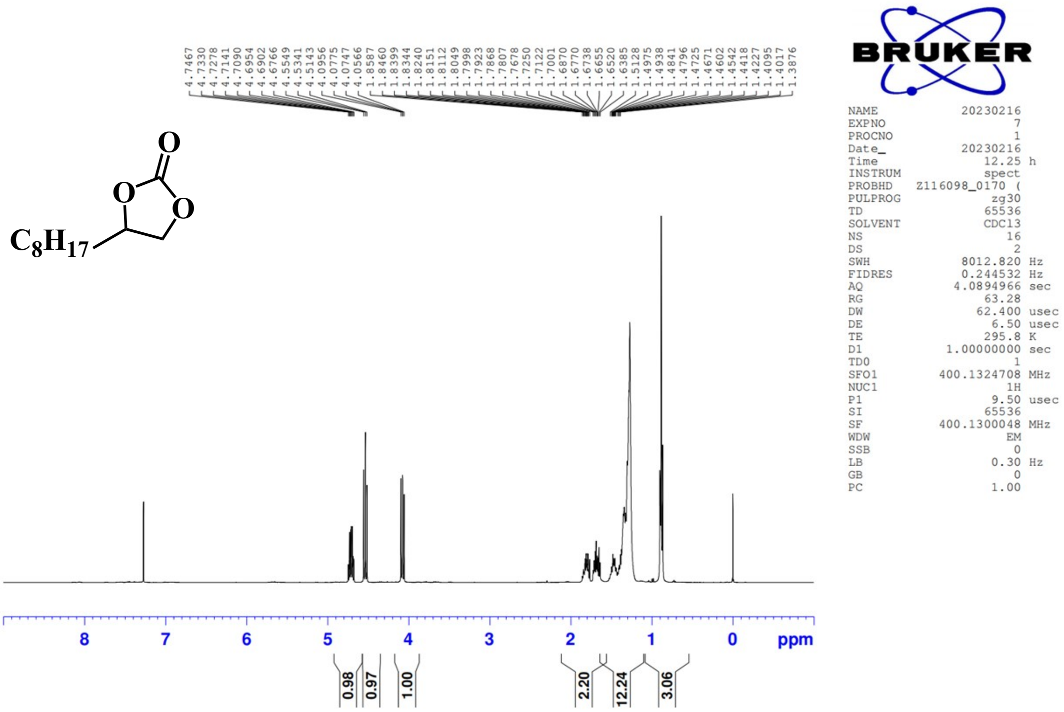

[1]H NMR (400 MHz, $CDCl_3$): δ 4.75 (m, 1H), 4.53 (t, 1H), 4.09 (q, 1H), 1.86 (m, 2H), 1.51 (m, 12H), 0.90 (t, 3H).

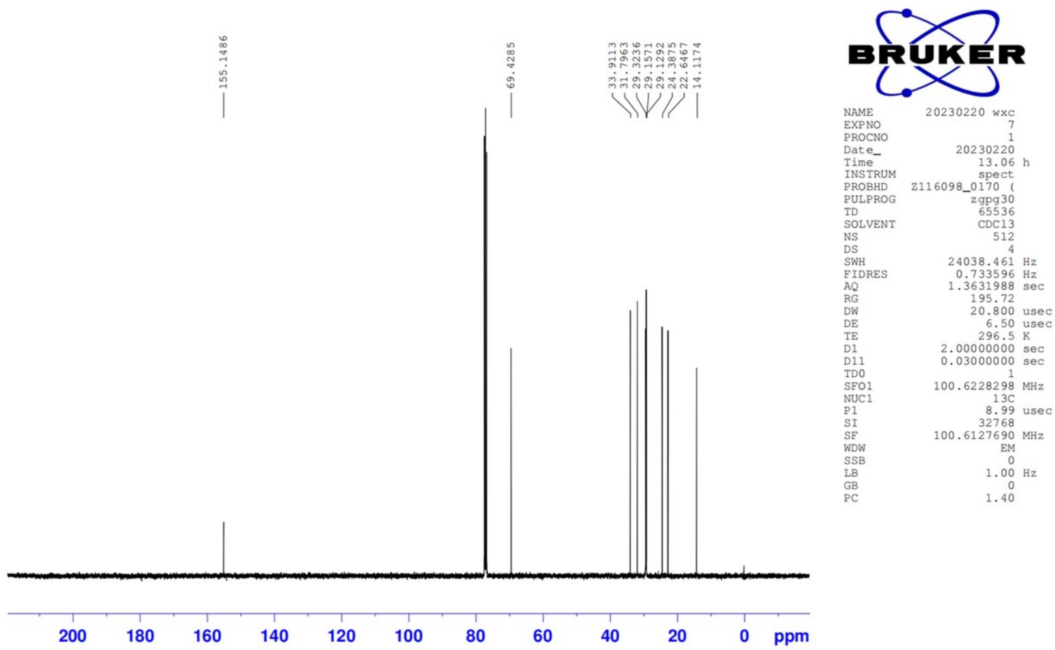

[13]C NMR (100 MHz, $CDCl_3$): δ 155.1, 77.1, 69.4, 33.9, 31.8, 29.3, 29.1, 29.1, 24.4, 22.6, 14.1.

4-decyl-1,3-dioxolan-2-one:

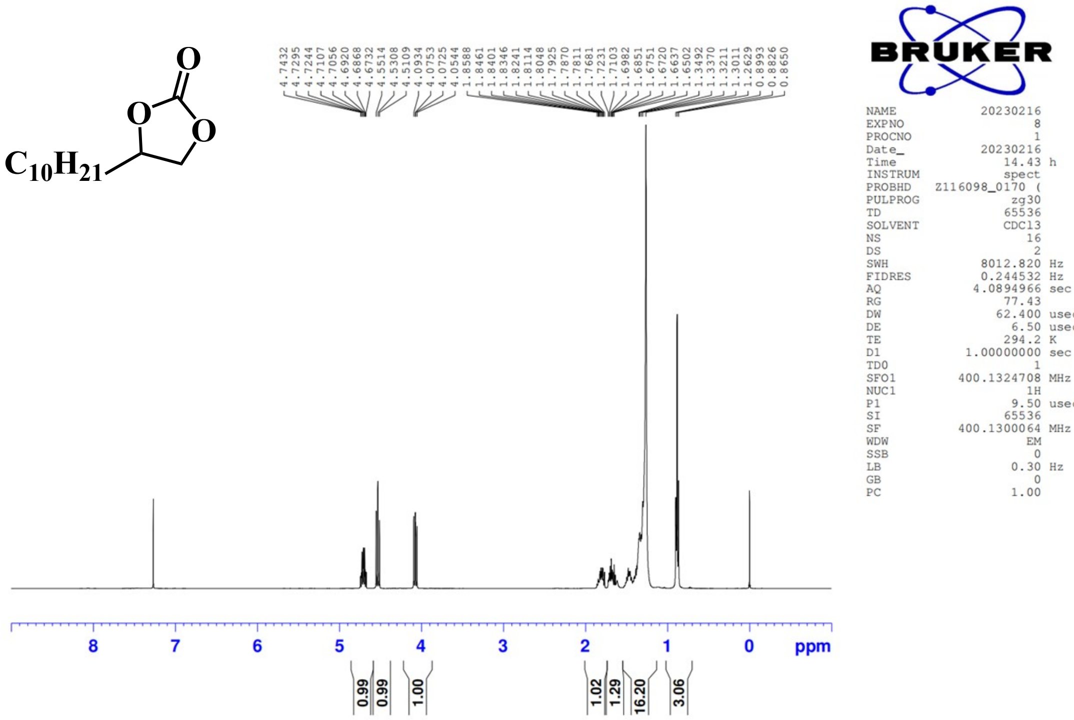

[1]H NMR (400 MHz, $CDCl_3$): δ 4.74 (m, 1H), 4.54 (t, 1H), 4.09 (t, 1H), 1.86 (m, 2H), 1.51 (m, 16H), 0.90 (t, 3H).

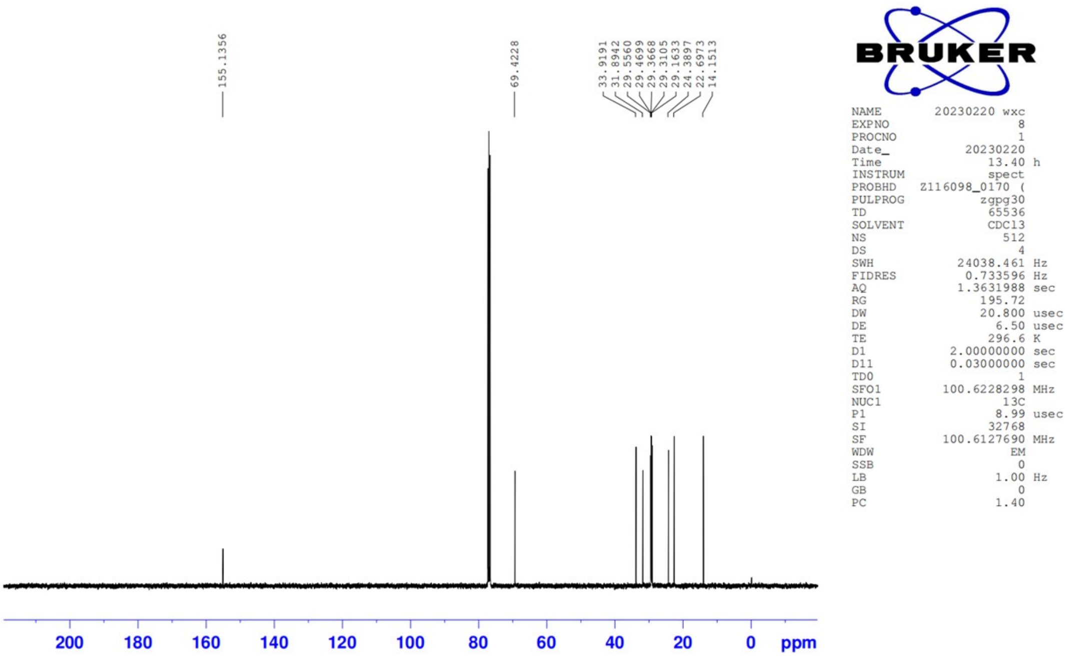

[13]C NMR (100 MHz, $CDCl_3$): δ 155.1, 77.0, 69.4, 33.9, 31.9, 29.5, 29.4, 29.3, 29.2, 29.1, 24.4, 22.7, 14.1.

4-dodecyl-1,3-dioxolan-2-one:

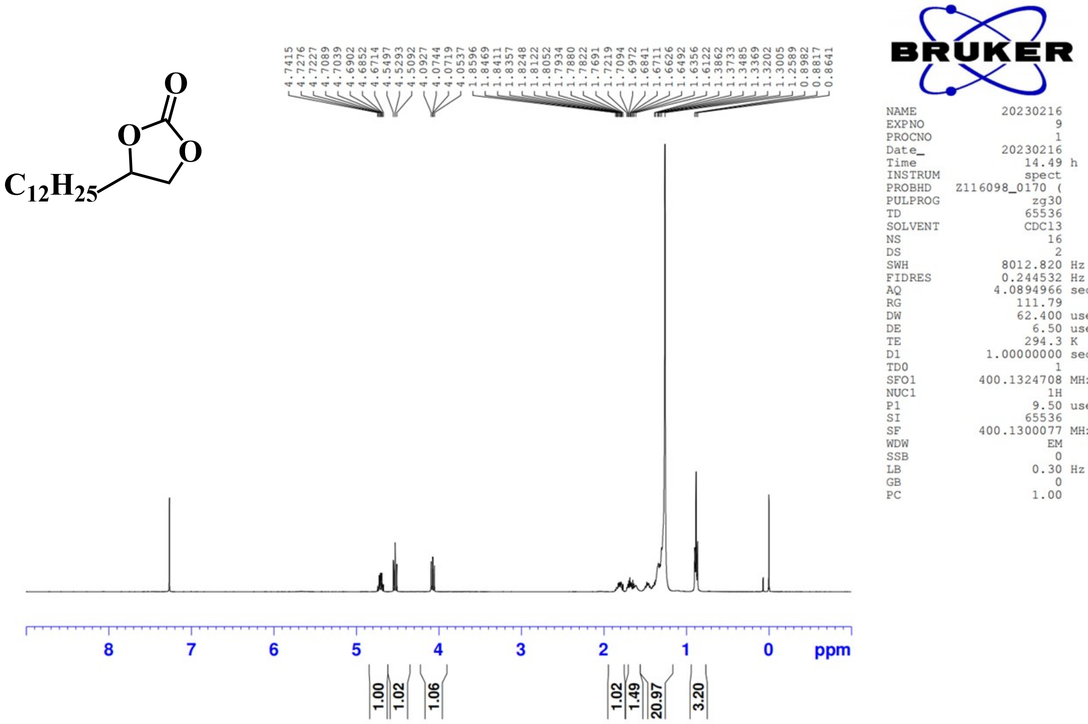

^{1}H NMR (400 MHz, $CDCl_3$): δ 4.74 (m, 1H), 4.54 (t, 1H), 4.09 (q, 1H), 1.85 (m, 2H), 1.51 (m, 20H), 0.90 (t, 3H).

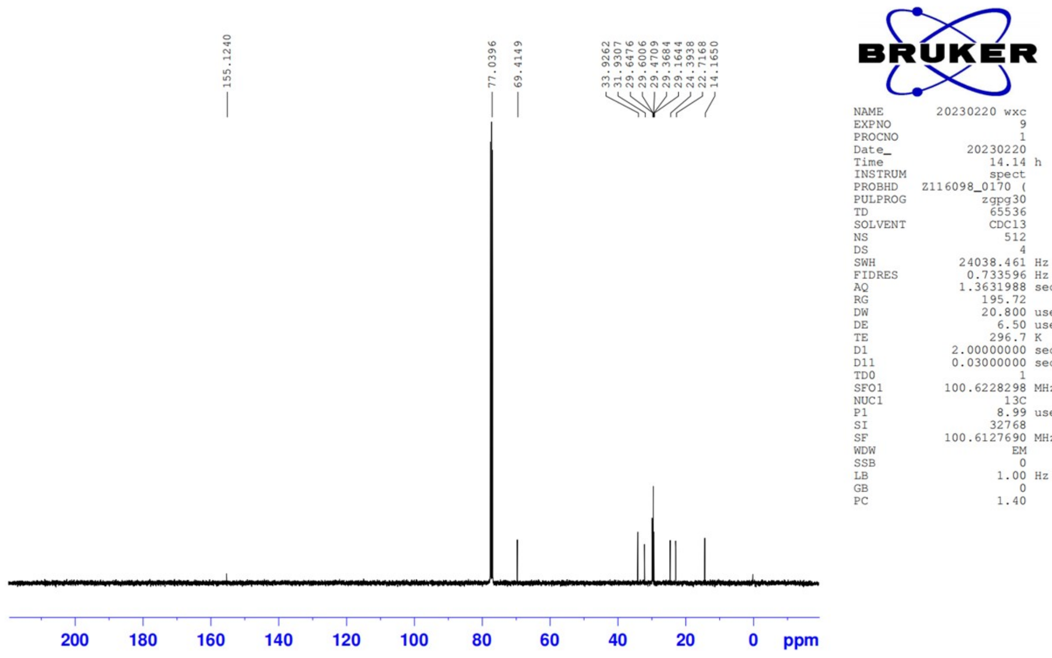

^{13}C NMR (100 MHz, $CDCl_3$): δ 155.1, 77.0, 69.4, 33.9, 31.9, 29.6, 29.6, 29.4, 29.3, 29.1, 24.4, 22.7, 14.1.

4, 5-cyclohexyl-1, 3-dioxolan-2-one

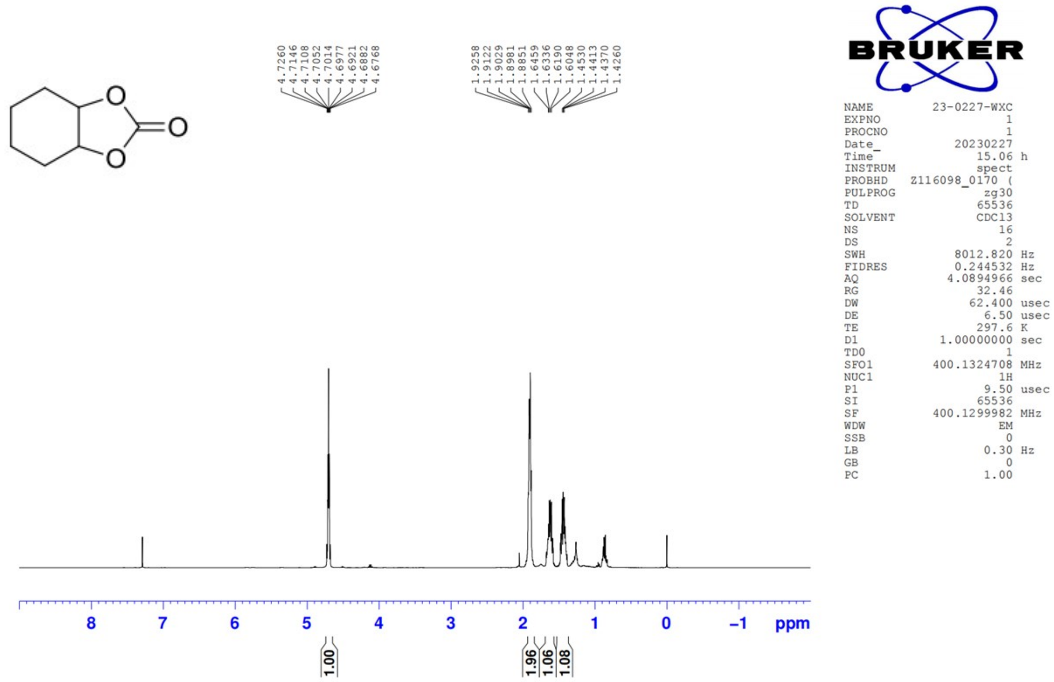

[1]H NMR (400 MHz, $CDCl_3$) δ 4.67 (m, 2H), δ1.88 (m, 4H), δ1.65(m, 2H), δ1.45(m, 2H).

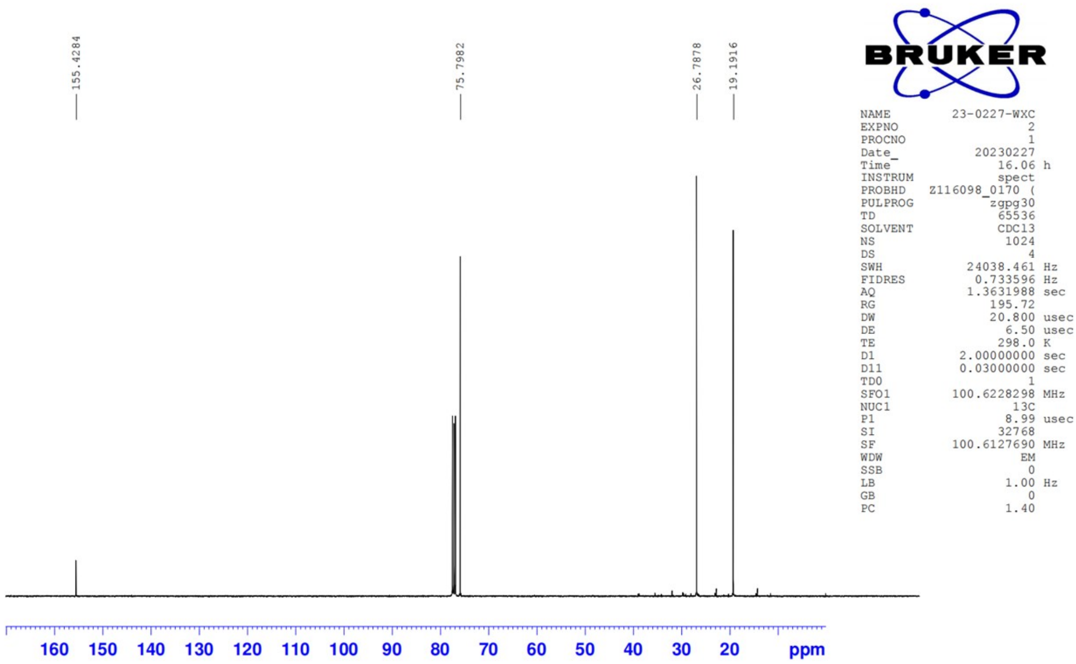

[13]C NMR (100 MHz, $CDCl_3$) δ 155.67, 76.05, 27.06, 19.45.

Supplementary References

1. S. Ghazali-Esfahani, H. Song, E. Păunescu, F. D. Bobbink, H. Liu, Z. Fei, G. Laurenczy, M. Bagherzadeh, N. Yan and P. J. Dyson, *Green Chem.* , 2013, **15**, 1584-1589.
2. X. Wang, Y. Zhou, Z. Guo, G. Chen, J. Li, Y. Shi, Y. Liu and J. Wang, *Chem Sci.*, 2015, **6**, 6916-6924.
3. I. Azcune, I. Garcia, P. M. Carrasco, A. Genua, M. Tanczyk, M. Jaschik, K. Warmuzinski, G. Cabanero and I. Odriozola, *ChemSusChem*, 2014, **7**, 3407-3412.
4. W. Zhong, F. D. Bobbink, Z. Fei and P. J. Dyson, *ChemSusChem*, 2017, **10**, 2728-2735.
5. Q. Sun, S. Ma, Z. Dai, X. Meng and F.-S. Xiao, *J. Mater. Chem. A*, 2015, **3**, 23871-23875.
6. Y. Xie, Q. Sun, Y. Fu, L. Song, J. Liang, X. Xu, H. Wang, J. Li, S. Tu, X. Lu and J. Li, *J. Mater. Chem. A*, 2017, **5**, 25594-25600.
7. Y. Xie, J. Liang, Y. Fu, M. Huang, X. Xu, H. Wang, S. Tu and J. Li, *J. Mater. Chem. A*, 2018, **6**, 6660-6666.
8. Z. Guo, X. Cai, J. Xie, X. Wang, Y. Zhou and J. Wang, *ACS Appl. Mater. Interfaces*, 2016, **8**, 12812-12821.
9. Y. Zhou, W. Zhang, L. Ma, Y. Zhou and J. Wang, *ACS Sustainable Chem. Eng.*, 2019, **7**, 9387-9398.
10. H. Song, Y. Wang, M. Xiao, L. Liu, Y. Liu, X. Liu and H. Gai, *ACS Sustainable Chem. Eng. ,* 2019, **7**, 9489-9497.
11. L. Qin, B. Wang, Y. Zhang, L. Chen and G. Gao, *Chem. Comm.* , 2017, **53**, 3785-3788.
12. Z. Guo, Q. Jiang, Y. Shi, J. Li, X. Yang, W. Hou, Y. Zhou and J. Wang, *ACS Catal.*, 2017, **7**, 6770-6780.
13. Y. He, D. Jiang, X. Li, J. Ding, H. Li, H. Wan and G. Guan, *J. CO_2 Util.* , 2021, **44**, 101427.
14. Q. Yi, T. Liu, X. Wang, Y. Shan, X. Li, M. Ding, L. Shi, H. Zeng and Y. Wu, *Appl. Catal., B*, 2021, **283**, 119602.
15. W. Hui, X.-M. He, X.-Y. Xu, Y.-M. Chen, Y. Zhou, Z.-M. Li, L. Zhang and D.-J. Tao, *J. CO_2 Util.* , 2020, **36**, 169-176.
16. J. Wang, W. Sng, G. Yi and Y. Zhang, *Chem Comm.*, 2015, **51**, 12076-12079.
17. J. Wang, J. G. Wei Yang, G. Yi and Y. Zhang, *Chem Comm.* , 2015, **51**, 15708-15711.
18. S. Xu, K. Song, T. Li and B. Tan, *J. Mater. Chem. A*, 2015, **3**, 1272-1278.
19. L. Hu, H. Ni, X. Chen, L. Wang, Y. Wei, T. Jiang, Y. Lü, X. Lu and P. Ye, *Polym. Eng. Sci.*, 2016, **56**, 573-582.
20. J. Li, D. Jia, Z. Guo, Y. Liu, Y. Lyu, Y. Zhou and J. Wang, *Green Chem.*, 2017, **19**, 2675-2686.
21. S. Hao, Y. Liu, C. Shang, Z. Liang and J. Yu, *Polym. Chem.*, 2017, **8**, 1833-1839.
22. P. Puthiaraj, S. Ravi, K. Yu and W.-S. Ahn, *Appl. Catal. B*, 2019, **251**, 195-205.
23. W. Zhang, F. Ma, L. Ma, Y. Zhou and J. Wang, *ChemSusChem*, 2020, **13**, 341-350.
24. X. Li, G. Chen and Q. Jia, *Microporous Mesoporous Mater.*, 2019, **279**, 186-192.
25. Y. Sang and J. Huang, *Chem. Eng. J.* , 2020, **385**, 123973.
26. J. Li, Y. Han, H. Lin, N. Wu, Q. Li, J. Jiang and J. Zhu, *ACS Appl. Mater. Interfaces*, 2020, **12**, 609-618.
27. D. Jia, L. Ma, Y. Wang, W. Zhang, J. Li, Y. Zhou and J. Wang, *Chem. Eng. J.*, 2020, **390**, 124652.
28. H. Zhou, Q. Chen, X. Tong and H. Liu, *Colloids Interface Sci. Commun* , 2020, **37**, 100285.
29. C. Liu, L. Shi, J. Zhang and J. Sun, *Chem. Eng. J.*, 2022, **427**, 131633.
30. H. Song, Y. Wang, Y. Liu, L. Chen, B. Feng, X. Jin, Y. Zhou, T. Huang, M. Xiao, F. Huang and H.

Gai, *ACS Sustainable Chem. Eng.*, 2021, **9**, 2115-2128.
31. Q. Ren, Y. Chen, Y. Qiu, L. Tao and H. Ji, *Cata. Lett.*, 2021, **151**, 2919-2927.
32. Y. Sang, Z. Shu, Y. Wang, L. Wang, D. Zhang, Q. Xiao, F. Zhou and J. Huang, *Appl. Surf. Sci.*, 2022, **585**, 152663.
33. X. Liao, B. Pei, R. Ma, L. Kong, X. Gao, J. He, X. Luo and J. Lin, *Catalysts*, 2022, **12**, 62.
34. K. Cai, P. Liu, T. Zhao, K. Su, Y. Yang and D.-J. Tao, *Microporous and Mesoporous Mater.*, 2022, **343**, 112135.
35. K. Wang, W. Cui, Z. Bian, Y. Liu, S. Jiang, Y. Zhou and J. Wang, *Appl. Catal., B*, 2021, **281**, 119425.
36. X. Suo, Y. Huang, Z. Li, H. Pan, X. Cui and H. Xing, *Sci. China Mater.* , 2021, **65**, 1068-1075.
37. X. Liao, X. Xiang, Z. Wang, R. Ma, L. Kong, X. Gao, J. He, W. Hou, C. Peng and J. Lin, *Sustainable Energy Fuels*, 2022, **6**, 2846-2857.
38. Y. Zhang, K. Liu, L. Wu, H. Huang, Z. Xu, Z. Long, M. Tong, Y. Gu, Z. Qin and G. Chen, *Dalton Trans.*, 2021, **50**, 11878-11888.
39. J. Gu, P. Shao, L. Luo, Y. Wang, T. Zhao, C. Yang, P. Chen and F. Liu, *Sep. Purif. Technol.*, 2022, **285**, 120377.
40. J. Cao, W. Shan, Q. Wang, X. Ling, G. Li, Y. Lyu, Y. Zhou and J. Wang, *ACS Appl. Mater. Interfaces*, 2019, **11**, 6031-6041.
41. S. Subramanian, J. Oppenheim, D. Kim, T. S. Nguyen, W. M. H. Silo, B. Kim, W. A. Goddard and C. T. Yavuz, *Chem*, 2019, **5**, 3232-3242.
42. L.-G. Ding, B.-J. Yao, F. Li, S.-C. Shi, N. Huang, H.-B. Yin, Q. Guan and Y.-B. Dong, *J. Mater. Chem. A*, 2019, **7**, 4689-4698.
43. J. Zhang, X. Li, Z. Zhu, T. Chang, X. Fu, Y. Hao, X. Meng, B. Panchal and S. Qin, *Adv. Sustain. Syst.* , 2020, **5**, 2000133.
44. G. Chen, Y. Zhang, J. Xu, X. Liu, K. Liu, M. Tong and Z. Long, *Chem. Eng. J.*, 2020, **381**, 122765.
45. Z. Xu, K. Liu, H. Huang, Y. Zhang, Z. Long, M. Tong and G. Chen, *J. Mater. Chem. A*, 2022, **10**, 5540-5549.